SEMMELWEIS EGYETEM

DOKTORI ISKOLA

Ph.D. értekezések

3444.

SZOTÁK-AJTAY KITTI

Celluláris és molekuláris élettan

című program

Programvezető: Dr. Hunyady László, egyetemi tanár

Témavezető: Dr. Jakus Zoltán Péter, egyetemi docens

IDENTIFICATION OF THE ORGAN-SPECIFIC FUNCTION OF LYMPHATICS: FOCUSING ON THE NEONATAL LUNG

PhD thesis

Kitti Szoták-Ajtay

Molecular Medicine Doctoral School

Semmelweis University

Supervisor: Dr. Zoltán Jakus, MD, Ph.D., Habil.

Official reviewers: Dr. Ákos Gasparics, MD, Ph.D.
Dr. Réka Vass, MD, Ph.D.

Head of the Complex Examination Committee:
Dr. Nándor Nagy, MD, Ph.D., Habil., D.Sc.

Members of the Complex Examination Committee:
Dr. Noémi Sándor, MD, Ph.D.
Dr. Zoltán Pós, MD, Ph.D.

Budapest
2026

Table of Contents

List of Abbreviations

α-SMA - alpha smooth muscle actin

ADAMTS3 - A disintegrin and metalloproteinase with thrombospondin motifs-3

AT2 - alveolar type 2

CC10 - club cell 10

CCBE1 - collagen and calcium binding EGF domains 1

Clp1 - cleavage factor polyribonucleotide kinase subunit 1

COPD - chronic obstructive pulmonary disease

c-JUN - jun proto-oncogene, AP-1 (activating protein-1) transcription factor subunit

DAPI - 4′,6-diamidino-2-phenylindole

DNA - deoxyribonucleic acid

ER - endoplasmic reticulum

ERK1/2 - extracellular signal-regulated kinase 1 and 2

FBM - fetal breathing movement

FGF10 - fibroblast growth factor 10

Flt4 - fms related receptor tyrosine kinase 4

GFP - green fluorescent protein

HE - hematoxylin-eosin

LYVE1 - lymphatic vessel endothelial hyaluronan receptor-1

LB - lamellar bodies

LECs - lymphatic endothelial cells

LNP - lipid nanoparticle

LPL - lysophospholipid

m1Ψ - one-methylpseudouridine

mRNA - messenger ribonucleic acid

Myf5 - myogenic factor 5

MyoD - myoblast determination protein 1

NG2 - neuron-glial antigen 2

PAS - periodic acid-Schiff

PCR - polymerase chain reaction

PDGFRα - platelet-derived growth factor receptor alpha

PDGFRβ - platelet-derived growth factor receptor beta

PDPN - podoplanin

PECAM1 - platelet and endothelial cell adhesion molecule 1

PROX1 - prospero homeobox protein 1

RDS- respiratory distress syndrome

RhD - rhodamine dextrane

RNA - ribonucleic acid

siRNA - short interfering ribonucleic acid

SP-A - surfactant protein A

SP-B - surfactant protein B

SP-C - surfactant protein C

SP-D - surfactant protein D

TonEBP - tonicity responsive enhancer binding protein

tRNA - transfer ribonucleic acid

TSEN - transfer ribonucleic acid splicing endonuclease

UTP - uridine-5′-triphosphate

VEGFC - vascular endothelial growth factor C

VEGFR3 - vascular endothelial growth factor receptor 3

YFP-yellow fluorescent protein

1. Introduction

1.1 Complex prenatal lung development program and respiratory disorders at birth

Prenatal lung development is crucial for the survival of mammalian newborns. To establish respiration, embryonic lungs must be inflated immediately after birth. This is a profound change, considering lungs develop in a fluid environment until this dramatic transition at the moment of birth. Lung development requires a complex prenatal pulmonary maturation program which prepares the lungs for air inflation and gas exchange at birth. Human lung development as described in the literature starts at 4 weeks of gestation with the appearance of the tracheal outgrowth from the foregut and the development continues until early childhood. Five distinct stages have been previously defined which overlap: embryonic (in human 4-7 weeks), pseudoglandular (in human 5-17 weeks), canalicular (in human 16-26 weeks), saccular (in human 24-38 weeks), and alveolar stage (in human 36 weeks-3 years) (Figure 1). In the embryonic stage the primary left and right lung buds appear and undergo branching to set up the overall lobular structure of the lung (1). At the end of the pseudoglandular stage the airway epithelial differentiation is occurring (2) and the complete structure of the human airway tree has been laid down (3). In this stage it has been reported that some fetal breathing movements (FBM) could appear at this time (10-11 weeks in human) as well (1, 4), it becomes regular and well-documented later in term. The epithelial differentiation and branching further continues in the canalicular stage. Furthermore, airways continue to increase in size and the most distal epithelial tubes widen and their surrounding mesenchyme thins. The first morphological signs of alveolar epithelial cell differentiation also appear at this time. In the saccular stage the branching morphogenesis end. Alveolar epithelial differentiation continues and importantly the surfactant system of the alveolar type 2 (AT2) cells matures. Surfactant production and lamellar bodies which are organelles specialized for the production and recycling of surfactant can be detected at this stage (1, 5) (Figure 2). The alveolar stage is characterized by the formation of the alveoli. The septa grow from the saccular walls to subdivide the distal saccules into alveoli. Therefore, the surface area for gas exchange is expanding (1). Meanwhile, microvascular maturation occurs and each capillary is completely surrounded by gas exchange surfaces (6).

Survival at birth is critical and much dependent on the adequate prenatal development and maturation of the lungs (1, 7-9). The leading causes of early neonatal morbidity are respiratory disorders, such as respiratory distress syndrome (RDS). The most described clinical symptoms of RDS are tachypnea, nasal flaring, irregular breathing, cyanosis, hypoxia etc. (10-14). It is a well-known data that there is a correlation between incidence and severity of RDS and the gestational weeks of the newborn. While the risk of RDS is very high (60%) in premature babies less than 28 weeks gestational age, than near-term infants, where this risk is 5% (15). The development of respiratory distress originates from the inefficiency of a neonate's lung to adapt to the new environment – as mentioned before – the change fluid to air. The last weeks of gestation are critical in preparing the fetus for the first breath. Late preterm infants are born in the late saccular stage of lung development when the antioxidant system and the surfactant production are still immature. Incomplete intrauterine maturation of the lung structure may lead to delayed intrapulmonary fluid absorption, surfactant insufficiency, and inefficient gas exchange (16).

Therapy of respiratory disorders, such as RDS mainly focuses on surfactant: the possible ways of surfactant substitution, stimulating and inducing surfactant production in preterm infants and newborns. Thus, large amounts of data are available about these therapies (17-20). Even though therapies targeting surfactant production and replacement vastly increased the survival of newborns with RDS, different aspects of lung development should be further studied to identify other possible therapeutic approaches. Studying lung development in any aspects is critical to better understand related diseases such as RDS and other respiratory disorders in neonates which can help find new ways in therapy as well.

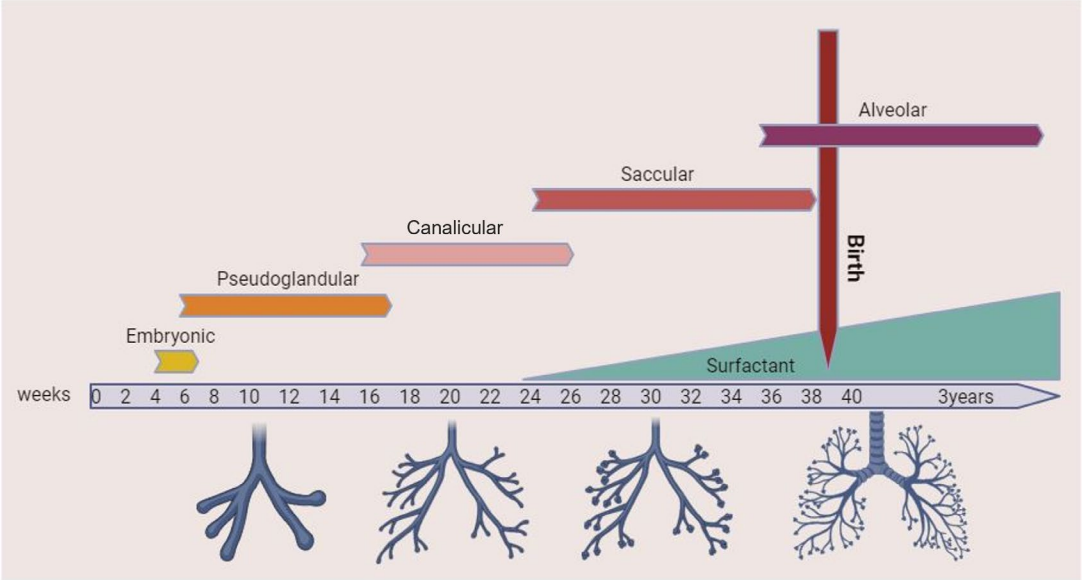

Figure 1 *Stages of lung development*

Five distinct stages of lung development: embryonic (in human 4-7 weeks), pseudoglandular (in human 5-17 weeks), canalicular (in human 16-26 weeks), saccular (in human 24-38 weeks), and alveolar stage (in human 36 weeks-3 years). Surfactant production starts at the saccular stage and it has a critical role in lung development. (1).

1.2 The role of surfactant in lung development

Lung surfactant has been described as a complex combination of components, which is produced by type II alveolar cells. It is stored in specialized structures called lamellar bodies, and exocytosed to the alveolar surface (21) (Figure 2). One crucial role of surfactant is to increase lung compliance by reducing surface tension in the lung (21-24). About 80% of the surfactant are phospholipids, which are synthesized in the endoplasmic reticulum (ER) of the type II alveolar cells and contains several classes, including: Phosphatidylcholine (75%), Phosphatidylglycerol (12%), Phosphatidylethanolamine (5%), Phosphatidylinositol (4%), Phosphatidylserine (2%), Sphingomyelin (1.5%), and Lysophospholipid (LPL) (<1%) (21, 25, 26). Surfactant also contains four proteins: surfactant protein A (SP-A), surfactant protein B (SP-B), surfactant protein C (SP-C), and surfactant protein D (SP-D), which are all produced by type II alveolar cells, however it has been reported that other airway cells, such as Club cells (CC10) and submucosal cells

synthetize these as well. The hydrophilic SP-A and SP-D participate in innate pulmonary immune defenses (21, 27) while the hydrophobic SP-B and SP-C interacts extensively with phospholipids of the surfactant and improves the lowering of the surface tension (21, 28). The only surfactant protein which is essential for survival is SP-B, thus the complete deficiency of it in mice and humans is lethal by causing neonatal RDS (29, 30). Furthermore, SP-B is essential for the packaging of phospholipids into lamellar bodies, the formation of tubular myelin, the processing of SP-C precursors and the establishment of a surfactant film to reduce surface tension (21, 31) (Figure 2). Lung surfactant also contains small amounts of neutral lipids, including cholesterol and it's esters, di-and triglycerides, and free fatty acids (26). However, the role of these neutral lipids in surfactant function has not been fully understood (21, 32, 33).

As mentioned before, the most documented and crucial functions of surfactant are to increase lung compliance, reduce surface tension, thus it facilitates neonatal lung inflation, and reduces the work required for breathing. Moreover, it helps maintaining the gas exchange area of the lungs (22, 24, 25). Surfactant also creates a nonspecific barrier against microorganisms by reducing adhesion and invasion into the lung (21, 34).

Surfactant is the main focus of therapies of respiratory disorders in preterm infants and newborns. Surfactant replacement was established as an effective and safe therapy for immaturity-related surfactant deficiency. It also improves pulmonary compliance, reduces RDS mortality and may lowers the risk of chronic lung disease (17-20). However, surfactant therapy also has limitations. Premature infants still require supportive care such as oxygen and mechanical ventilation which could cause long-term complications (35, 36). Therefore, the need for other therapeutic methods and target mechanisms arise which could help in the therapy of respiratory disorders and also to improve our understanding of the preparation of the developing lung for inflation at birth.

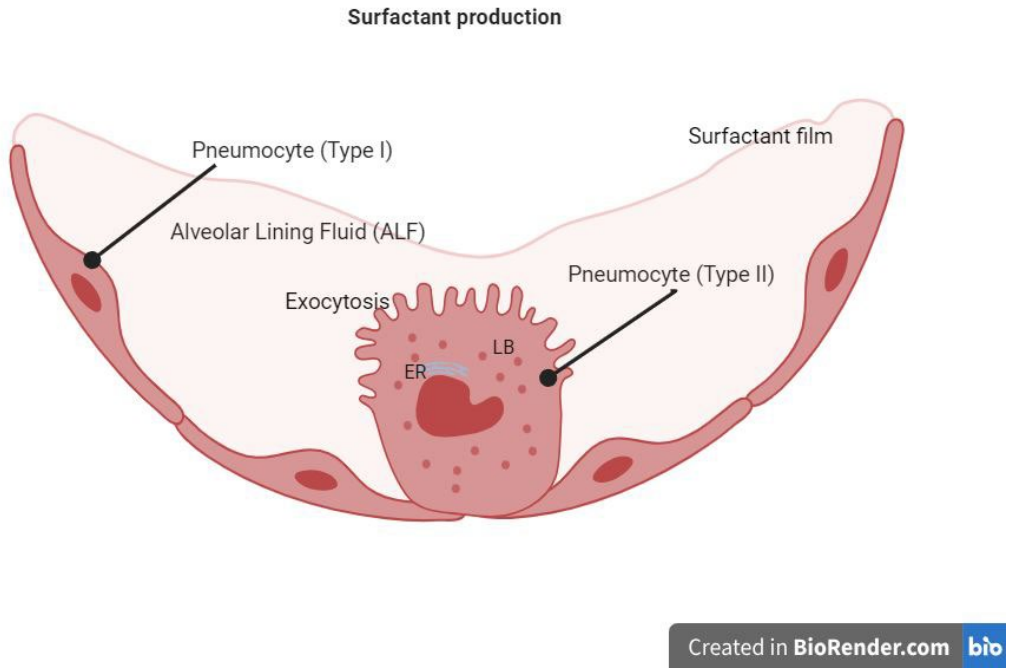

Figure 2 *Schematic representation of surfactant production*

Surfactant is synthesized in the endoplasmic reticulum (ER) of type II alveolar cells and stored in specialized structures called lamellar bodies (LB) then exocytosed. Figure was created based on (21).

1.3 Lymphatic system

The immaturity of the newborns lung structure is one of the main factors in the development of respiratory distress, where one pathogenic factor is the delayed intrapulmonary fluid absorption (16). One of the best-known function of the lymphatic system is the maintenance of the tissue homeostasis via interstitial fluid drainage. Therefore, it has been indicated that the lymphatic system might have a role in preparing the newborn lung for the first breath.

The lymphatic vasculature starts as an open capillary network which beside maintaining tissue homeostasis is also essential in the defense against pathogens. Therefore, tissues such as the skin and mucous membranes, which are often exposed to foreign antigens, are especially rich in lymphatic vessels. In recent years it has become increasingly clear that the lymphatic system has organ-specific functions as well. It has been described that the lymphatics partake in the intestinal lipid absorption and are present in the central nervous system (37). It is well documented in animal models that

the lymphatic vessels begin draining interstitial fluid at the late gestational period in the lung (38) (Figure 3).

The lymphatic system consists of lymphatic capillaries, collecting lymphatic vessels and lymph nodes. Lymphatic capillaries which have button-like junctions between lymphatic endothelial cells (LECs), uptake interstitial fluid and macromolecules. It drains into collecting lymphatic vessels, which are present in the bronchovascular bundles and interlobular septa in the lung. The collecting lymphatic vessels have tighter and continuous zipper-like junctions. In most organs they are covered with smooth muscle cells that provide lymph flow. In contrast, the collecting lymphatics in the lung lack this smooth muscle cell coverage (39, 40). The lymph then drains into the thoracic lymph nodes, and eventually into the thoracic duct, here the lymph is returned to the blood circulation.

In the past it was a challenge to visualize lymphatic vessels, thus it has been historically ignored in research. Early anatomic studies mainly depended on intravascular injection of contrast agents. However, there was a revolution in the visualization of lymphatic endothelial cells (LECs) during the late 1990s when lymphatic-specific markers were identified (41). These markers were vascular endothelial growth factor receptor (VEGFR)-3 (42, 43), prospero homeobox 1 (PROX1) transcription factor (26), integral membrane glycoprotein podoplanin (PDPN) (44), and lymphatic vessel endothelial hyaluronan receptor 1 (LYVE1) (45). As a result, research of the lymphatic system gained immense scientific interest during the last decades. Moreover, new findings have discovered unexpected perspectives to research regarding the lymphatic vasculature (41).

Vascular endothelial growth factor C (VEGFC) and its receptor, vascular endothelial growth factor receptor 3 (VEGFR3) which is coded by the fms related receptor tyrosine kinase 4 (*Flt4*) gene, are key molecules in lymphangiogenesis. Loss of function of VEGFC or VEGFR3 blocks lymphatic development in fish and mice (46, 47) and one of the underlying factors for human primary lymphedema syndromes (48, 49). A disintegrin and metalloproteinase with thrombospondin motifs-3 (ADAMTS3) protease and collagen and calcium binding EGF domains 1 (CCBE1) are involved in the catalysis of VEGFC processing (Figure 4) (50, 51). In vivo studies indicated that CCBE1 has a critical role in the processing of the active form of the lymphangiogenic factor VEGFC in mouse skin (51, 52).

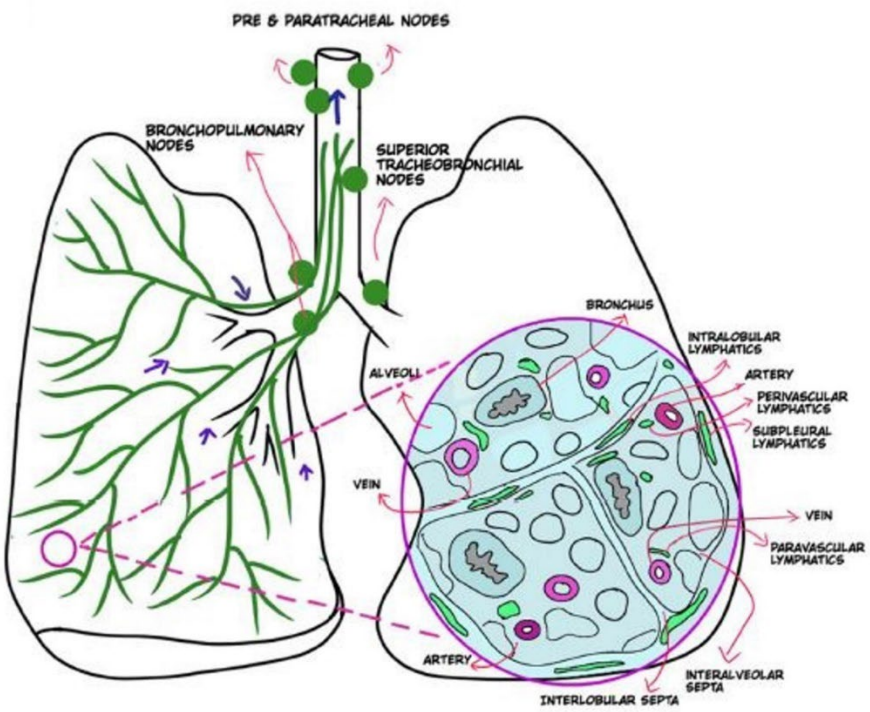

Figure 3 *Lymphatic vessels in the healthy lung*

Structure of the lymphatics in the lung (green, left). Arrows indicating the direction of lymph flow. Cross section of the lung (right) and the distribution of lymphatics in relation to other lung structures. Trivedi and Reed (43)

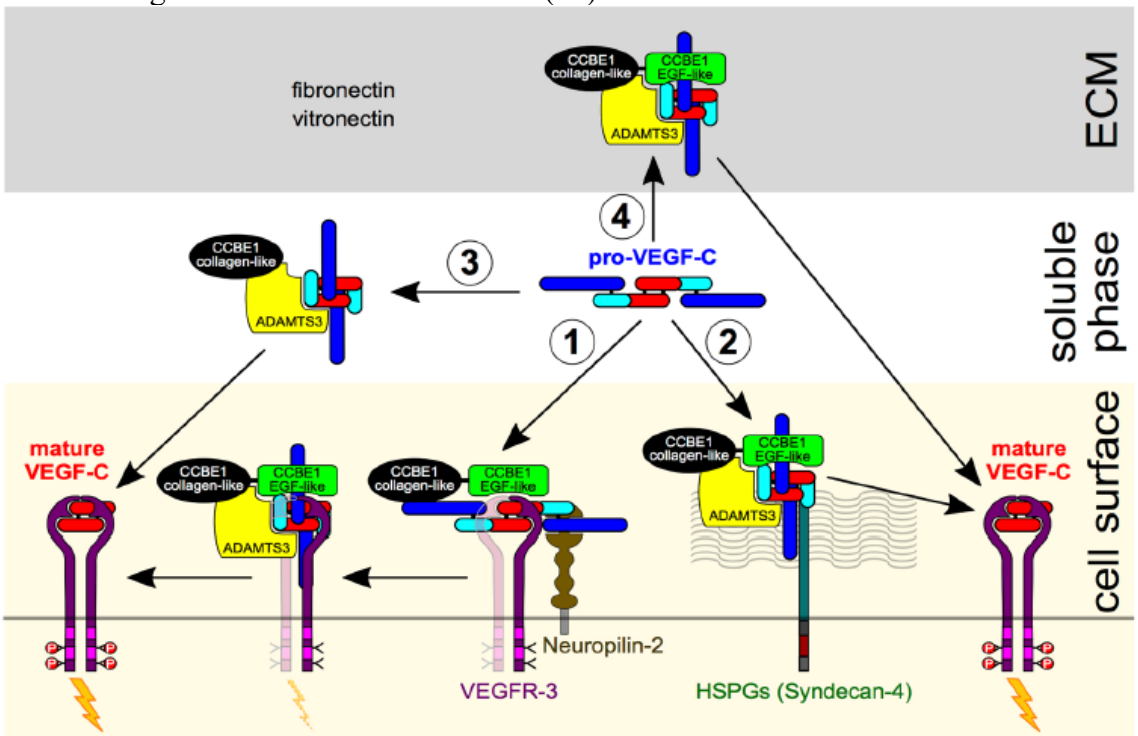

Figure 4 Schematic view of VEGF-C activation based on Jha et al 2019 (51).

Proteolytic cleavage of pro-VEGF-C simultaneously activates and mobilizes VEGF-C. Jha et al. propose four different modes of VEGF-C activation: 1. Activation of VEGFR-3-bound VEGF-C16; 2. Activation of Heparan Sulfate Proteoglycan (HSPG)-bound VEGF-C18; 3. Activation of VEGF-C in the soluble phase11; and 4. Activation of extracellular matrix (ECM)-bound VEGF-C. After proteolytic activation, VEGFR-3-bound VEGF-C can immediately start signaling (activation mode #1), while HSPG-bound VEGF-C18 first needs to translocate to VEGFR-3 (activation mode #2).The role of CCBE1 is twofold: It accelerates the proteolytic cleavage and localizes pro-VEGF-C to efficiently form the trimeric activation complex (51).

1.4 Role of lymphatic function in preparation for the first breath

Lungs develop in a fluid environment in utero, the removal of this fluid and the inflation of the lung immediately after birth are critical steps. The removal of fluid from the lung starts before birth (53, 54). An experiment with lambs and sheep in 1977 concluded that pulmonary lymph flow was higher in newborn lambs than adult sheep. It was concluded that this difference was the result of a higher filtration pressure and an increased vascular surface area for fluid exchange in newborn lambs compared to adult sheep (55). However, a few years later the same research group reported that lung lymph flow and lymph protein flow were not significantly different in late gestation fetal lambs and newborn lambs (54). In conclusion, these early studies do not entirely explain the role of lymphatics in prenatal lung. However, prior study of our research group has reported that lymphatic function has a role in preparing the lung for inflation at birth which experiment will be described in detail later (38).

Lymphatic endothelial transcription factor PROX1 (56), the lymphangiogenic factors VEGFC (46), CCBE1 (57), the lymphatic endothelial growth factor receptor VEGFR3 (58, 59) among other factors are essential for lymphatic development, therefore their damage or loss results impaired development or even total absence of the lymphatics. It is also reported that all mice lacking lymphatics die shortly after birth (46, 56-59). However, the exact mechanism requires further research. To study this question in a previous study (38) our research group investigated newborn and late gestation CCBE1-defficient mice (*Ccbe1*$^{-/-}$). CCBE1-deficient newborns appeared severely cyanotic and died shortly after birth while control (*Ccbe1* $^{+/+}$, *Ccbe1*$^{+/-}$) newborns appeared healthy, their skin was of pink color consistent with normal tissue oxygenation within 5–20 min and were viable. Of note, *Ccbe1*$^{-/-}$ newborns had normal diaphragms and exhibited gasping and costal retractions which show normal neuromuscular function and respiratory

drive. This shows that CCBE1-deficient mice lacking lymphatics exhibit respiratory failure and die immediately after birth. Moreover, kinase-dead VEGFR3 *(Vegfr3$^{kd/kd}$)* newborn mice, which also lack lymphatics, show the same phenotype, but not wild-type or *Vegfr3$^{kd/+}$* neonates (they were viable, pink colored). However, these findings do not explain the lymphatics-dependent molecular and cellular mechanisms involved in late gestational lung development. Lungs of newborn cyanotic *Ccbe1$^{-/-}$* and *Vegfr3$^{kd/kd}$* mice sank when placed in saline while non-cyanotic *Ccbe1$^{-/-}$* and *Vegfr3$^{kd/kd}$* lungs floated. This suggests that mice lacking lymphatic function are unable to inflate their lungs after birth. These studies also described that the failure of lung inflation is not due to surfactant deficiency. Importantly, measurement of the total lung compliance of E18.5 *Ccbe1$^{-/-}$ and Vegfr3$^{kd/kd}$* lungs revealed significant decrease in compliance compared to control littermates. All in all, these experiments revealed that lymphatic function increases lung compliance before birth, and contributes to the successful inflation of the lung and also changes lung mechanics to prepare for inflation at birth (38).

In addition to all known data there are still many questions related to lung development, especially preparation for the first breath. However, these findings raise the possibility of other mechanisms participating in preparing the developing lung for inflation at birth. Fetal breathing movements (FBMs), which we know little of, is a mechanism that may be involved in this process.

1.5 Fetal breathing movements (FBM)

During in utero development fetuses perform breathing like movements in multiple species, including humans and mice, (60). These are the so-called fetal breathing movements (FBMs), which are contractions of the respiratory muscles with differing amplitude and frequency. FBMs begin in humans from approximately 10-11 weeks of gestation (4, 61). Breathing movements slowly increase with the gestational age (4, 62, 63), and become regular in the second and third trimester. These are also more frequent as term ends. However, the percentage of time spent breathing can vary widely (64). Little is known about the physiological role of FBMs that are available in literature. It is known that FBMs are responsible for spontaneously decreasing intrathoracic pressure and expanding the fetal lung during intrauterine life. It has been reported that FBMs are a marker of the maturation of the central nervous system which is involved in controlling

respiratory muscles (61, 64-67). In general, fetal breathing supports lung development, strengthens respiratory muscles, and is claimed to fine-tune the neural circuitry that drives breathing. (60, 68-70). However, currently the exact role of the fetal breathing movements is still not fully known.

1.6 Prior experimental approaches to study FBMs have great limitations

The first hypothesis was that blocking or the lack of fetal breathing movements or prolonged leakage of amniotic fluid causes pulmonary hypoplasia, which often cause high morbidity and mortality (71-75). In early studies, the deficiency or absence of FBMs has been reported to possibly be in connection with decreased proliferation and increased apoptosis of pulmonary cells in the hypoplastic lungs (71, 72, 75).

Early studies of FBMs were surgical approaches where the spinal cord or phrenic nerve were disrupted in animal models, although these heroic surgical interventions had influenced a number of other physiological processes in addition to the FBMs (76, 77). Ferwell and colleagues reported that the phrenic nerve section eliminated fetal breathing movements and resulted in decreased airway fluid volume, lung weight, and total lung deoxyribonucleic acid (DNA) (77) in lambs. However, the research group of Bamford did a similar experiment where they concluded that both the phrenic nerve denervated and sham operated groups had smaller lungs with lower water content (76). Thus, these surgical experiments lead to conflicting results and had serious limitations as these interventions influenced a number of physiological processes that interfered with the study of the role of FBMs.

Another method to study FBMs is the drainage of the amniotic fluid where not only FBMs but also the volume and function of the organs are affected (78-80). In the study of Alcorn et al. (78) chronic drainage of intrauterine lung fluid led to reduced lung weight and it was concluded that this intervention inhibited fetal lung growth. In another study in one lamb one lobe was drained and the other lobe was ligated leading to fluid retention. The drained side showed hypoplasia while the ligated one exhibited hyperplasia (80). In conclusion, in these experiments not only the FBMs but also the volume and function of the organs were affected which presents limitations to conclude that these findings are solely due to the disruption of FBMs.

Embryos paralyzed from the early embryonic period have severe defects of the skeletal development represented in their smaller size and reduced growth (71, 72, 75). Tseng et al. (75) used myogenin null mouse embryos, which lacked normal skeletal muscle fibers thus skeletal muscle movements in utero. They found that the total lung DNA of these embryos has decreased as well as the body weight ratio (75). In the studies of Inanlau and Kablar myogenic factor 5 deficient (*Myf5*$^{-/-}$) mice embryos and *Myf5*$^{-/-}$:*MyoD*$^{-/-}$ (myoblast determination protein 1) double knock out mouse embryos were used (71, 72). Myogenic factor 5 (Myf5) protein (which coded by Myf5 gene) has a major role in regulating muscle differentiation or myogenesis, specifically the development of the skeletal muscle. (81, 82). *Myf5*$^{-/-}$ embryos lacked the rib cage and functional intercostal musculature therefore the lack of fetal breathing movements was present and these embryos suffered from pulmonary hypoplasia due to the reduced number of proliferating lung cells and due to the increased number of terminal deoxynucleotidyl transferase. Data showed the absence of pulmonary expansion and lung development was stopped in the canalicular stage in these embryos (71). MyoD is a transcription factor and it has a key role in regulating muscle differentiation (83). The *Myf5*$^{-/-}$:*MyoD*$^{-/-}$ double knock out mouse embryos had no skeletal muscles including main respiratory muscles (82) and had even more severe phenotype characterized by elevated lung apoptotic index. Furthermore, the development and differentiation of type I and type II pneumocytes was damaged as well in these embryos (72), which presents as being a crucial limitation of these experiments. In summary, these experiments studied the role of FBMs in mouse embryos with extreme impairment of the skeletomuscular system from an early embryonic stage, and the findings on lung development are limited and not fully conclusive on the FBMs as the immense systemic developmental impairments could also influence respiratory development.

In conclusion, all these prior experimental approaches have major limitations. Therefore, there is a great need to develop new methods to better understand the role of FBMs in preparation for the first breath.

1.7 *Clp1*$^{K/K}$ mouse strain as a model

Josef M. Penninger and his research group described the kinase-dead cleavage factor polyribonucleotide kinase subunit 1 (*Clp1*$^{K/K}$) mouse model (84). Cleavage factor

polyribonucleotide kinase subunit 1 (CLP1) proteins are kinases and participate in multiple ribonucleic acid (RNA) pathways. Furthermore, as CLP1 associates with the transfer ribonucleic acid (tRNA) splicing endonuclease (transfer ribonucleic acid splicing endonuclease (TSEN)) complex, they have a role in the splicing tRNA precursors (85). Loss of CLP1 kinase activity results in the accumulation of RNA fragments, aberrant processing of pre-transfer RNAs and induce p53-dependent cell death (84). Late gestation $Clp1^{K/K}$ mice show a progressive loss of spinal motor neurons associated with axonal degeneration and denervation of neuromuscular junctions, resulting in impaired motor function, muscle weakness, paralysis and fatal respiratory failure (84). It is shown that all newborn $Clp1^{K/K}$ mice and E18.5 embryos exhibited a lordotic body posture and dropping forelimbs, indicative of impaired motor functions (84). Importantly, the reexpression of wild type (WT) CLP1 rescues the motor neuron loss and genetic inactivation of p53 rescues $Clp1^{K/K}$ mice from the motor neuron loss (84). The $Clp1^{K/K}$ newborns (on the c57Bl/6 genetic background) die shortly after birth caused by fatal respiratory failure. These findings raise the question whether lung development is affected in this mouse model. Therefore, they investigated lung development and morphogenesis which appeared to be normal according to Caveolin 1, Surfactant protein A and Surfactant protein C expression (84).

Overall, kinase-dead Clp1 mice represent an ideal genetic model for investigating the role of FBMs, given that skeletomuscular development remains unaffected and respiratory muscle denervation occurs only during late gestation.

1.8 Investigation of lymphatics in the skin

As new studies are presented, it has become gradually clear that lymphatic vessels, present in different organ-specific environments, have organ specific functions as well as classical functions. So, to further characterize the organ specific roles of lymphatic function, next to the lung, as a second big topic, the lymphatic growth of the skin was in our interest.

Skin is especially rich in lymphatic vessels and capillaries which play a key role in maintaining tissue fluid balance. In skin, superficial lymphatic capillaries expand into the dermal papilla where they collect interstitial fluid and drain into the collecting lymphatic vessels (86). Here the lymphatic vessels are comprised of lined together endothelial cells.

These endothelial cells interact with each other through adhesion junctions (VE-cadherin/β-catenin complex) and tight junctions, and with the extracellular matrix through integrins (87, 88). The lymphatic vessels anchor to the extracellular matrix and lack a continuous basement membrane. Overlapping flaps of endothelial cells of lymphatic capillaries lack junctions at the tip but are anchored on the sides by discontinuous button-like junctions (39).

The dysfunction of the lymphatic system contributes to the pathogenesis of various diseases and defects which can lead to lymph accumulation in tissues. When abnormal accumulation of interstitial fluid happens caused by impaired lymphatic drainage it is defined as lymphedema. Primary and secondary lymphedemas can be distinguished by pathogenesis. Primary lymphedemas are inherited diseases and are the result of defects in genes of lymphatic vessel development. Secondary lymphedema is caused by the damage of lymphatic vessels most commonly due to surgery, infections or radiation therapy (41, 89). Due to the accumulation of extracellular fluid, swelling is present at affected areas, and lymphedema may result in recurrent local bacterial and fungal infections and can lead to fibrosis (89, 90) which all results in decreased function of affected organs, tissues and therefore degrades quality of life. Currently used therapeutic approaches are comprised of manual lymph drainage or compression therapy, however these have great limitations, their effectiveness is poor and only provide symptomatic relief (91). All considered, there is an immense need for new therapeutic methods to provide more effective treatment to reduce symptoms or cure this disease.

Another aspect is that during aging of the skin, the number of lymphatic vessels decreases, and their function reduces, which is related to the decreased adhesion junctions between lymphatic endothelial cells, especially VE-cadherin. VEGFC/VEGFR-3 signaling pathway plays an important role in the remodeling and expansion of lymphatic vessels; downregulation of this pathway contributes to the dysfunction of the lymphatic system (86).

However, there are still open questions, and better understanding of the function of lymphatics in the skin is needed to improve treatment of related diseases. As written earlier, Vascular Endothelial Growth Factor C (VEGFC) is the most important lymphangiogenic factor, which induces VEGFR3-dependent lymphatic growth (46, 92, 93). Recently one of the most promising novel therapeutic platform developed is the

nucleoside-modified messenger ribonucleic acid (mRNA) encapsulated in lipid nanoparticles (LNPs) (94) which has established safety and efficacy for a vast range of applications in numerous preclinical models (95-98). This new platform has numerous advantages. RNA molecules do not integrate into the host genome which is an important advantage for future therapeutic purposes as well. Moreover, there is no anti-vector immunity after repeated administrations in the host. The protein production of modified mRNA is highly controllable. Furthermore, the manufacturing is rapid, scalable, and sequence-independent which does not require complex and expensive infrastructure (96).

Searching for new tools in the therapy of lymphedema we hypothesized whether the mRNA-LNP platform with VEGFC encoding mRNAs could be an effective tool to induce the growth of lymphatics in the skin.

2. Objectives

Our goals were to define and to characterize the role of FBMs in the neonatal lungs and develop a new approach to study the role of lymphatic in adult skin.

I. In the neonatal lung in addition to surfactant and lymphatic function we aimed to investigate other mechanisms which may play role in preparation of the developing lung for inflation at birth. Since the physiological importance of fetal breathing movements (FBMs) is not clear, our aim was to define the physiological role of FBMs in preparation for air inflation of the prenatal lung at birth. For that we used the *Clp1*$^{K/K}$ mouse strain as a genetic model which has denervation of skeletal muscles during late gestation. Here we determined the following aims:

1. Our aim was to characterize the phenotype of *Clp1*$^{K/K}$ mouse strain.
2. Next, we aimed to describe lung development in *Clp1*$^{K/K}$ embryos compared to control.
3. We also wanted to characterize the lymphatic function in late gestation embryos lacking FBMs.

II. Identificating organ-specific function of lymphatics, next to the neonatal lung, our goal was to investigate lymphatic growth in the skin. We aimed to develop a system to induce organ-specific lymphatic growth in the skin. Since VEGFC is one of the most important growth factor of lymphatics and mRNA-LNP platform is a potent new therapeutic tool for protein production, our aim was to investigate and characterize whether nucleoside-modified VEGFC mRNA-LNPs could effectively induce the growth of new lymphatic vessels in the skin of adult mice. New findings would improve our knowledge and therapy of lymphedemas, for which at this moment only symptomatic treatments are available. Investigations of lymphatic growth in the skin with nucleoside-modified VEGFC mRNA-LNPs presented in this thesis are part of another series of experiments. This aligns with the current thesis by investigating the organ-specific functions of lymphatics, studies in which I participated.

3. Methods

3.1 Animals

Mice carrying the kinase-dead Clp1 allele (*Clp1*^{K}) (84) were maintained on c57Bl/6 genetic background. Embryos and newborns of heterozygous matings were genotyped by allele-specific polymerase chain reaction (PCR) using 5'-TTG GTT CAG GTA TTA AGT CGT TGG-3'forward and 5' GAA TTG CAT AGT CTT TCC TCC ATC-3' reverse primers. *Flt4*^{YFP} (*Flt4* promoter-driven expression of yellow fluorescent protein) mice (99) were crossed to *Clp1*$^{K/+}$ animals and maintained in heterozygous form on the c57Bl/6 background. Offsprings were genotyped by allele-specific PCR primer sets including 5' GGA TCA CTC TCG GCA TGG AC-3' forward and 5'-GGG CGT CCT CAT ACC TAG GT-3' reverse primers (I).

To investigate lymphatic vessels in the skin, 6–12-week-old Prox1^{GFP}(prox1 promoter-driven expression of green fluorescent protein)) lymphatic reporter animals obtained from the Mutant Mouse Regional Resource Centers were maintained in heterozygous form and genotyped by a transgene-specific PCR using 5′ - GAT GTG CCA TAA ATC CCA GAG CCT AT – 3′ forward and 5′ – GGT CGG GGT AGC GGC TGA A – 3′ reverse primers (100) (II).

Experimental animals were housed in either conventional or specific pathogen free animal facilities. All animal experiments were approved by the Animal Experimentation Review Board of Semmelweis University and Government Office for Pest County (Hungary). Licenses of the experiments are PEI/001/404-8/2015, PE/EA/148-4/2018 PE/EA/1654-7/2018.

3.2 Timed Matings and Handling of Late Gestation Embryos and Newborns

Clp1$^{K/+}$ heterozygous animals were used to set up overnight timed matings. To examine prenatal lung development and morphology before air exposure and extra-uterine respiratory changes, the embryos were sacrificed in utero by immersing the gravid uterus into ice-cold phosphate-buffered saline (PBS) for 40 minutes before harvesting the embryos from the uterus under fluid as described before (38) (I).

Embryos were collected at E14.5, E15.5, E16.5, E17.5, E18.5 and E19.5. Cesarean sections were performed at E19.5 followed by rapid removal of the embryos from the

uterus and their manual stimulation. Naturally born and cesarean section newborns were monitored for 2 hours after birth and scored after 20-30 minutes. Thereafter, tail samples were collected for genotyping, and tissues were harvested from the embryos and newborns. The whole chest, isolated lungs, gut and skin were used for histology, weight and DNA content measurements (I).

3.3 Histological Processes and Immunohistochemistry for Neonatal Lung Experiments

Embryonic and newborn tissues were fixed in 4% paraformaldehyde (Sigma-Aldrich) overnight on 4°C, dehydrated in 50, 70, 95 and 100% ethanol, then embedded in paraffin using a Leica EG1150H embedding station. Seven micrometer-thick sections were generated using an HM340E Thermo Scientific microtome and processed for hematoxylin-eosin (HE) (Leica), periodic acid-Schiff (PAS) (Sigma-Aldrich), trichrome (Sigma-Aldrich) and immunohistochemistry staining. The following primary antibodies were used for immunostaining: anti-LYVE1 (R&D Systems, AF2125), anti-PROX1 (Angiobio, 11-002P), anti-VEGFR3 (R&D, AF743) anti-CC10 (Santa Cruz Biotechnology, Inc., sc-9772), anti-SP-C (Merck, AB3786), anti- alpha smooth muscle actin (anti-α-SMA) (Abcam, ab124964), anti-Desmin (Dako, M0760), anti-PDPN (R&D Systems, AF3244), anti-platelet-derived growth factor receptor alpha (anti-PDGFRa) (Cell Signaling Technology, 3164), anti-platelet-derived growth factor receptor beta (anti-PDGFRb) (Cell Signaling Technology, 3169), anti-Vimentin (Cell Signaling Technology, 5741), anti-platelet and endothelial cell adhesion molecule 1 (anti-PECAM1) (R&D Systems, MAB3628), and anti-neuron-glial antigen 2 (anti-NG2) (EMD Millipore, AB5320). As secondary antibodies Alexa Fluor 488 and 568 conjugated anti-goat or anti-rabbit antibodies (Life Technologies) were used. As a nucleus staining 4′,6-diamidino-2-phenylindole (DAPI) containing mounting medium (Vector Laboratories) was used. Microscopic images were taken by a Nikon ECLIPSE Ni-U microscope connected to a Nikon DS-Ri2 camera. Alveolar area (averaging 8–10 fields of view per embryo) and septal thickness (averaging 80–100 measurements per embryo), lymphatic vessel area (average of all visible pulmonary lymphatic vessels per embryo per section and normalized for the mean area of the littermate controls) measurements were performed in NIS-Elements Imaging Software (Nikon) using a 40x dry objective (40x

images). Different structures and cell types of immunofluorescent images were quantified using Fiji software (101) (I).

3.4 DNA Content Measurements

For total DNA content measurements DNA was isolated from whole lungs of *Clp1*$^{K/K}$ and littermate control E18.5 embryos using DNeasy blood and tissue isolation kit (Qiagen). DNA concentration of the whole lungs was measured by NanoDrop OneC Microvolume UV–Vis Spectrophotometer (Thermo Scientific) (I).

3.5 Monitoring Pulmonary Lymphatic Function *in vivo*

To monitor lymphatic function, mice carrying the kinase-dead Clp1 allele were crossed to *Flt4*^{YFP} mice. *Clp1*$^{K/+}$ females and *Clp1*$^{K/+}$ males were time mated. Pregnant *Clp1*$^{K/+}$ females were anesthetized. 0.5 µl of 70 kDa rhodamie-dextrane (RhD) (Life Technologies) at 10 mg/ml concentration was injected through the uterus and chest wall into the lung of E18.5 *Clp1*$^{K/K}$ and littermate control embryos on *Flt4*^{YFP} lymphatic reporter background as described before (38, 102). Selective uptake and transport of large molecular weight RhD in fluorescent reporter positive lymphatic vessels were monitored 60 minutes after the injection by a fluorescent Nikon SMZ25 stereomicroscope equipped with Nikon DS-Ri2 camera. To quantify the transport of fluorescently labeled macromolecules, the intensity of the RhD signal was measured in NIS-Elements Imaging Software (Nikon) in reporter positive lymphatic vessels (the background intensity was subtracted). Then the tissue samples were collected for genotyping (I).

3.6 Design, production of VEGFC mRNAs and LNP formulation of Poly(C) and VEGFC mRNAs

Norbert Pardi from University of Pennsylvania, Perelman School of Medicine, Philadelphia, PA, USA designed and produced the nucleoside-modified mRNAs. Barbara L. Mui, Ying K. Tam, Thomas D. Madden and Michael J. Hope from Acuitas Therapeutics, Vancouver, BC, Canada developed and prepared the lipid nanoparticles. mRNAs were produced by using T7 RNA polymerase (Megascript, Ambion) on linearized plasmids encoding codon-optimized mouse VEGFC (pTEV-muVEGFC-A101). mRNAs were transcribed to contain 101 nucleotide-long poly(A) tails. One-

methylpseudouridine (m1Ψ)-5′-triphosphate (TriLink) instead of uridine-5′-triphosphate (UTP) was used to generate modified nucleoside-containing mRNA. RNAs were capped using the m7G capping kit with 2′-O-methyltransferase (ScriptCap, CellScript) to obtain cap1. Poly(C) (Sigma-Aldrich) and murine VEGFC-encoding mRNAs were encapsulated in LNPs using a self-assembly process in which an aqueous solution of mRNA at pH =4.0 is rapidly mixed with a solution of lipids dissolved in ethanol (II).

3.7 Monitoring in vivo lymphatic growth in the skin of adult mice

6–12-week-old Prox1^{GFP} lymphatic reporter mice were intradermally injected with 1 µg of Poly(C) (Control) or VEGFC mRNA-LNPs into the back skin. In parallel experiments contralateral injections were performed into the right and left sides of the same animal in these experiments. After 22 days the animals were sacrificed, and tissues were harvested. Lymphatic growth in lymphatic reporter animals was visualized by fluorescent stereo microscopy using a Nikon SMZ25 microscope connected to a Nikon DS-Ri2 camera. For paraffin-based histology the back skin was fixed in 4% paraformaldehyde (Sigma-Aldrich) overnight on 4°C, dehydrated in 50, 70, 95 and 100% ethanol, then embedded in paraffin using a Leica EG1150H embedding station. Seven micrometer-thick sections were generated using a HM340E Thermo Scientific microtome processed for immunohistochemistry staining. Anti-LYVE1 (R&D Systems, AF2125) primary antibody and Alexa Fluor 568 conjugated anti-goat secondary antibody (Life Technologies) were used for immunostaining. As a nucleus staining DAPI containing mounting medium (Vector Laboratories) was used. Microscopic images were taken by a Nikon ECLIPSE Ni-U microscope connected to a Nikon DS-Ri2 camera (II).

3.8 Presentation of Data and Statistical Analysis

Experiments were performed the indicated number of times. Macroscopic pictures and microscopic images are representative of three or more independent experiments. For all experiments, investigators were blinded by the origin of embryos and newborns until the end of the analysis. NIS-Elements Imaging (Nikon), Fiji Software (NIH), and Adobe Photoshop were used for image processing and analysis. Results are shown as mean and SEM. For statistical analysis GraphPad Prism 7.0 and Microsoft Office Excel software programs were used. Specific statistical tests are presented in the figure legend for each

experiment. *P-values* <0.05 were considered statistically significant. Figures 1-3 were created on BioRender.com.

4. Results

4.1 *Clp1*$^{K/K}$ Embryos and Newborns Exhibit Impaired Skeletal Muscle Function Including FBMs

To characterize the phenotype of *Clp1*$^{K/K}$ embryos and newborns we set up timed matings. As expected, and others shown before (84) after birth mice carrying two kinase dead CLP1 alleles (*Clp1*$^{K/K}$) exhibited impaired respiration and motility, or a complete lack of breathing and movement. *Clp1*$^{K/K}$ newborns were cyanotic and presented signs of acute respiratory failure and died shortly after birth. While control *Clp1*$^{+/+}$ mice showed normal breathing, movement and color (Figure 4A). The weight and size of Clp1$^{K/K}$ and *Clp1*$^{+/+}$ control mice showed no difference (Figure 4A, B). HE stained lung sections of *Clp1*$^{K/K}$ newborns show reduced alveolar area and thickened alveolar wall compared to the *Clp1*$^{+/+}$ littermate controls (**P = 0.0090 for alveolar area and **P = 0.0030 for septal thickness) (Figure 4C–E).

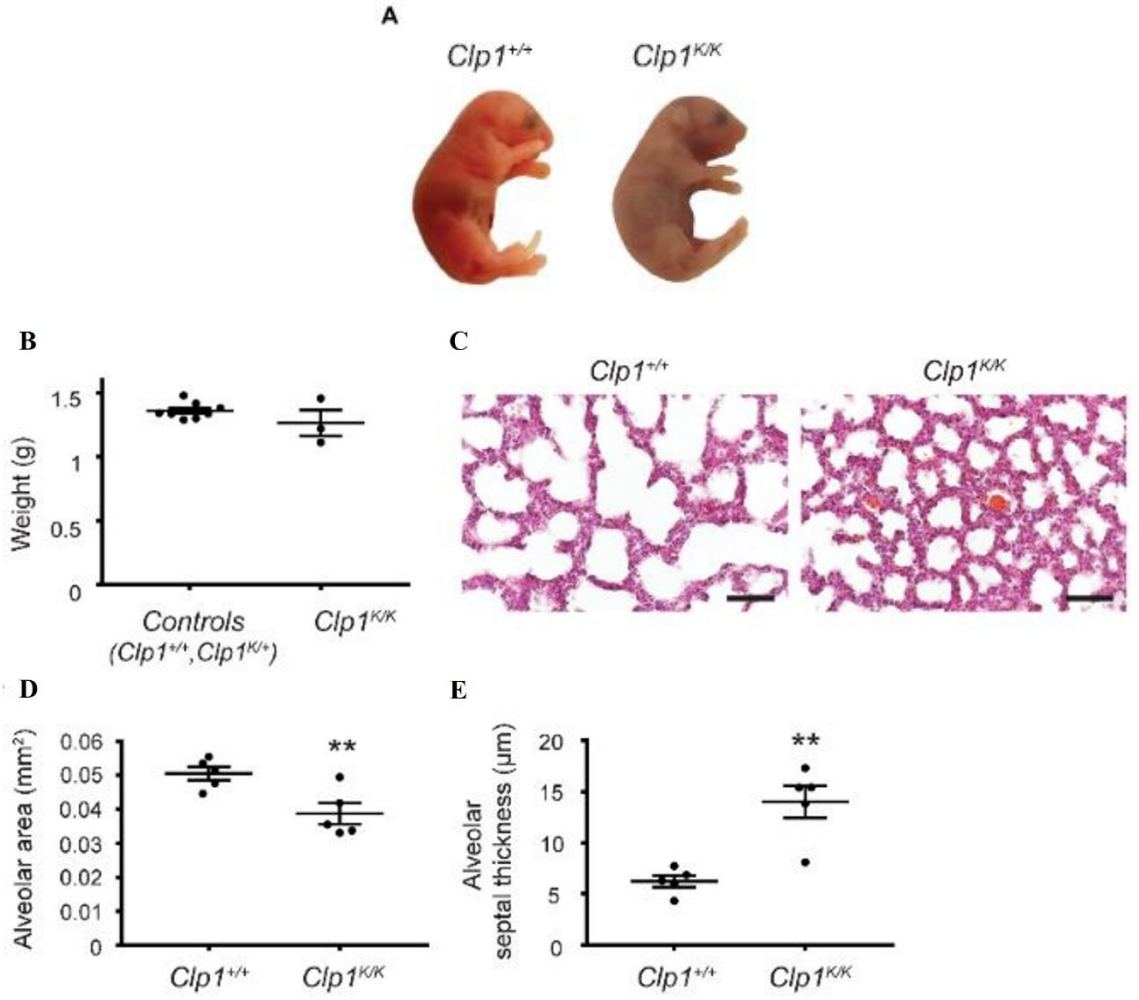

Figure 4 *Clp1$^{K/K}$ mice with impaired skeletal muscle activity develop respiratory failure and die after birth (I).*

A) Appearance of newborn *Clp1$^{+/+}$* and *Clp1$^{K/K}$* littermates on a c57Bl/6 genetic background. Representative images are shown of 15-19 embryos from 6 litters. **B**) Total weight of control (*Clp1$^{+/+}$* or *Clp1$^{K/+}$*) and *Clp1$^{K/K}$* newborns. Quantitative data are shown as mean and SEM of 3-8 embryos from 1 litter (P=0.187 (two-tailed t-test)). **C**) Representative images of lung morphology shown by HE staining of newborn *Clp1$^{+/+}$* and *Clp1$^{K/K}$* littermates on the c57Bl/6 background 60 min after birth. Representative images are shown of 5 newborns of each group. Bars, 50µm. **D-E**) Quantitative data for alveolar area and alveolar septal thickness are represented in newborn lungs of *Clp1$^{+/+}$* and *Clp1$^{K/K}$* littermates on a c57Bl/6 genetic background (mean and SEM, n=5 per group, **P<0.01 (two-tailed t-test)).

4.2 Late Gestation *Clp1*$^{K/K}$ Embryos Do Not Show Altered Expression of Molecular and Cellular Markers of Lung Development

Next, we characterized the expression of molecular markers of late lung development in *Clp1*$^{K/K}$ and *Clp1*$^{+/+}$ mice on the c57Bl/6 genetic background before birth. Their expression levels were normal; these included CC10 (Club cell 10), alveolar type II cells (SP-C-surfactant protein c), type I cells (PDPN-podoplanin), mesenchyme (platelet-derived growth factor receptor alpha (PDGFRα), Vimentin, Desmin), vascular smooth muscle cells and pericytes (platelet-derived growth factor receptor beta (PDGFRβ), NG2, and α-SMA), lung endothelial cells (PECAM1) (Figure 5). Pulmonary LECs stained with markers, VEGFR3, PROX1, and LYVE1 showed normal expression levels with no major difference in the number of cells or vascular structures in *Clp1*$^{K/K}$ compared to control *Clp1*$^{+/+}$ mice shown by representative images (Figure 5). However, the only difference we observed was the dilation of lymphatic vessels in *Clp1*$^{K/K}$ late gestation embryos compared to the controls (*Clp1*$^{+/+}$) shown by LYVE1, PROX1, and VEGFR3 lymphatic markers (Figure 5).

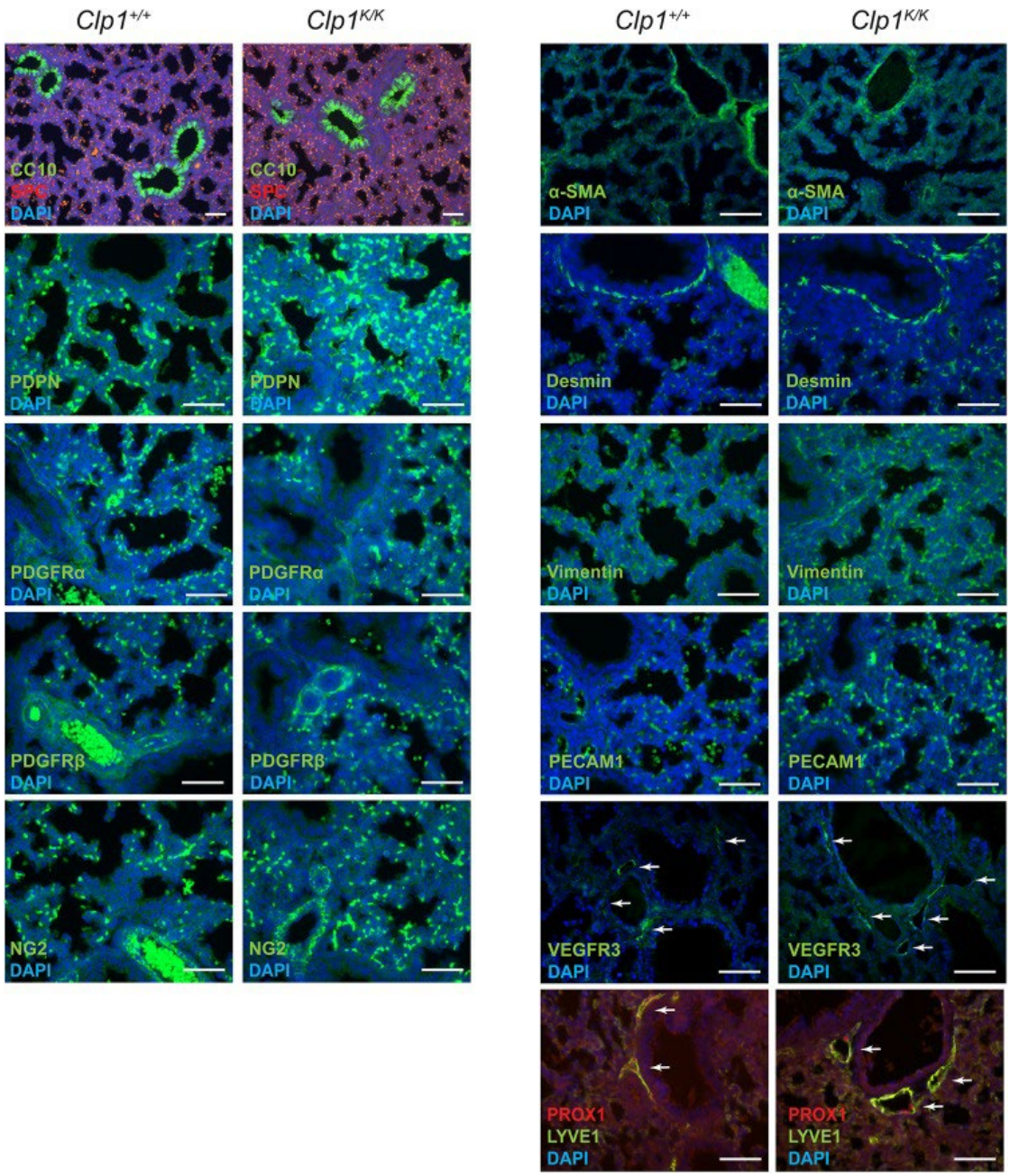

Figure 5 *No difference in molecular and cellular lung development in late gestation Clp1$^{K/K}$ embryos compare to controls (I).*

Immunostaining for CC10, SP-C, PDPN, PDGFRα, PDGFRβ, NG2, α-SMA, Desmin, Vimentin, PECAM1, VEGFR3, LYVE1, PROX1 and DAPI nuclear staining are shown in late gestation lungs of *Clp1*$^{+/+}$ and *Clp1*$^{K/K}$ embryos at E18.5. Representative images are shown of 3-5 independent experiments per group. Bars, 50µm.

4.3 Late Gestation Lung of *Clp1*$^{K/K}$ Embryos Show Thickened Alveolar Septum and Reduced Alveolar Area Before Air Inflation

We characterized the lungs of *Clp1*$^{K/K}$ and *Clp1*$^{+/+}$ embryos in each embryonic day from E14.5 to birth by HE stained sections to study the possible impact of FBMs on the structure of the developing lungs. It revealed no detectable changes before E16.5 in *Clp1*$^{K/K}$ embryos in the examined parameters. However, at E17.5 we observed thickened alveolar septum and reduced alveolar area in *Clp1*$^{K/K}$ embryos compared to control *Clp1*$^{+/+}$ embryos. These changes were detectable at E18.5 and E19.5 as well (*P = 0.0165 for alveolar area and **P = 0.0018 for septal thickness at E17.5 and *P = 0.0103 for alveolar area and *P = 0.0348 for septal thickness at E18.5) (Figure 6A–C). To further confirm normal lung development, we performed PAS and trichrome staining (Figure 6F, G). Trichrome staining would reveal fibrosis but that was not the case. We could not detect any difference between *Clp1*$^{K/K}$ and control late gestation lungs (Figure 6F). PAS staining revealed normal levels of glycogen in the alveolar cells of *Clp1*$^{K/K}$ embryonic lungs at E18.5 (Figure 6G). DNA content and dry weight of *Clp1*$^{K/K}$ embryonic lungs were also normal at E18.5 (P = 0.1753 for DNA content and P = 0.1452 for dry weight) (Figure 6D, E). These findings are consistent with our molecular results supporting normal growth and maturation of lung cell types.

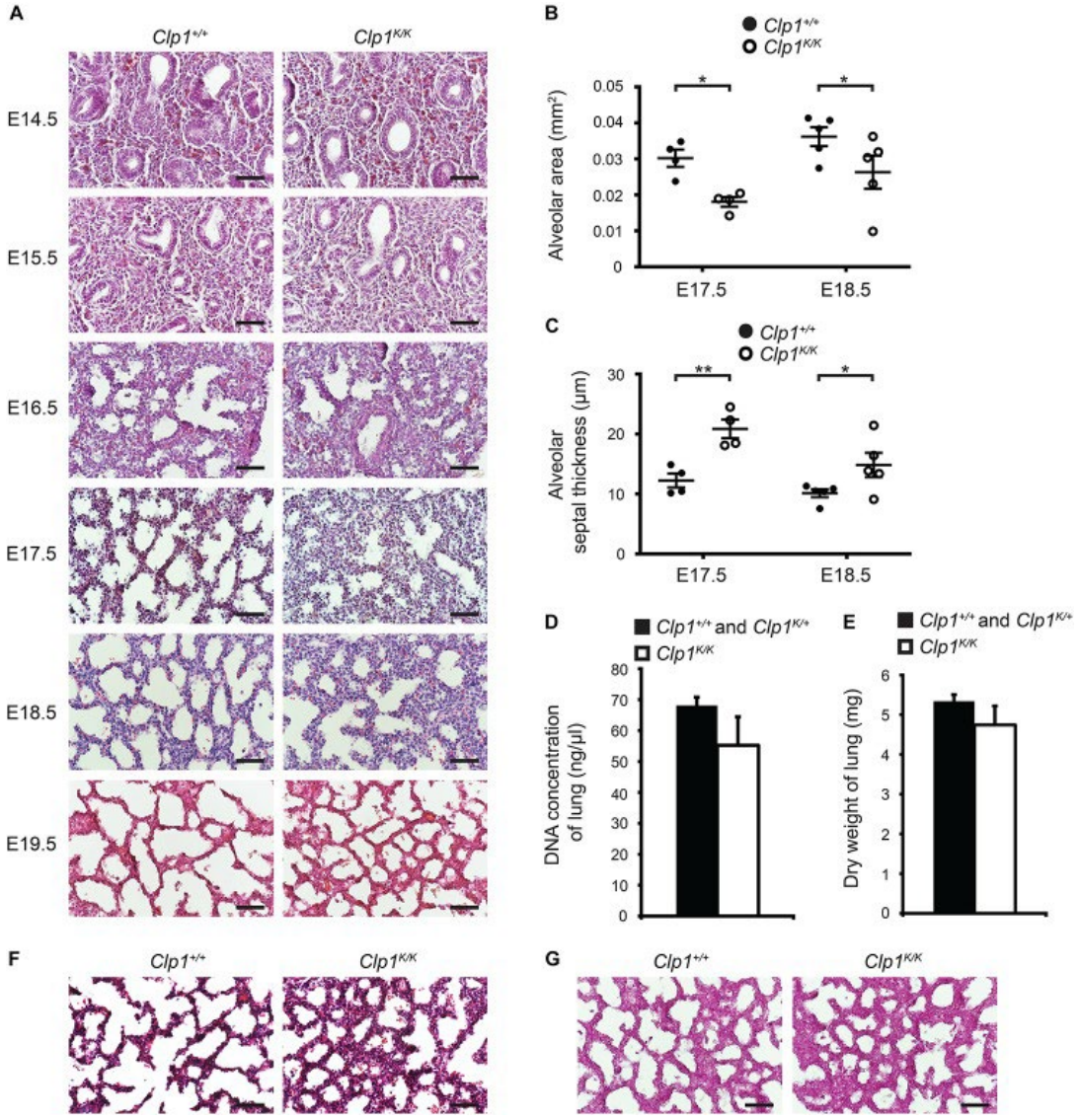

Figure 6 *Thicker alveolar septum and reduced alveolar area in $Clp1^{K/K}$ mice with impaired FBMs before air inflation of the lung (I).*

A) Morphology of embryonic lungs shown by HE histology of $Clp1^{+/+}$ and $Clp1^{K/K}$ embryos before air inflation in utero at E14.5, E15.5, 16.5, E17.5, E18.5 and E19.5 on the c57Bl/6 genetic background. Representative images are shown of 2-4 embryos per group from 1-2 litters. Bars, 50µm. **B-C**) Quantitative data for alveolar area and alveolar septal thickness of $Clp1^{+/+}$ and $Clp1^{K/K}$ embryonic lungs (E17.5 and E18.5) on the c57Bl/6 genetic background. Quantitative data are represented as mean and SEM from 4-5 embryos in each group (*P<0.05,**P<0.01, (two-tailed t-test)). **D**) Total DNA content of the lungs shown as DNA concentration in late gestation control ($Clp1^{+/+}$, $Clp1^{K/+}$) and $Clp1^{K/K}$ embryos at E18.5. Quantitative data are shown as mean and SEM from 5-6 embryos in each group (P=0.1752748, (two-tailed t-test)). **E**) Dry weights of late gestation lungs of control ($Clp1^{+/+}$, $Clp1^{K/+}$) and $Clp1^{K/K}$ embryos at E18.5. Quantitative data are shown as mean and SEM from 5-17 embryos in each group (P= 0,14519 (two-tailed t-test)). **F-G**) Trichrome staining (**F**) and Periodic acid-Schiff (PAS) staining (**G**) for levels of the surfactant precursor glycogen and fibrotic proteins in the lungs of $Clp1^{+/+}$

and *Clp1*$^{K/K}$ embryos at E18.5. Representative images are shown of 3 embryos examined in each group. Bars, 50 μm.

4.4 The Pulmonary Lymphatic Vessels Are Markedly Dilated in Late Gestation *Clp1*$^{K/K}$ Embryos Before Air Inflation

To describe pulmonary lymphatic growth in *Clp1*$^{K/K}$ embryos we investigated embryos at different time points from E14.5 to E19.5 and performed immunohistochemistry with lymphatic markers. It revealed that lymphatic vessels appeared at E14.5 and developed normally in the *Clp1*$^{K/K}$ embryos as well as control *Clp1*$^{+/+}$ embryos (Figure 7A). Importantly at late gestation, at E17.5, E18.5, E19.5 lymphatic vessels appeared to be dilated in the *Clp1*$^{K/K}$ mice compared to the *Clp1*$^{+/+}$ mice (Figure 7A, B). However, in other organs such as small intestine and skin, the structure of lymphatic vessels showed no difference at E17.5, E18.5, E19.5 in the *Clp1*$^{K/K}$ compared to the *Clp1*$^{+/+}$ control embryos (Figure 7C).

To summarize, lymphatic vessels develop normally in *Clp1*$^{K/K}$ mice and in controls as well. Although in the *Clp1*$^{K/K}$ mice the structure of lymphatic vessels showed dilation compared to the controls, which may indicate damaged function of pulmonary lymphatics (Figure 7A, B).

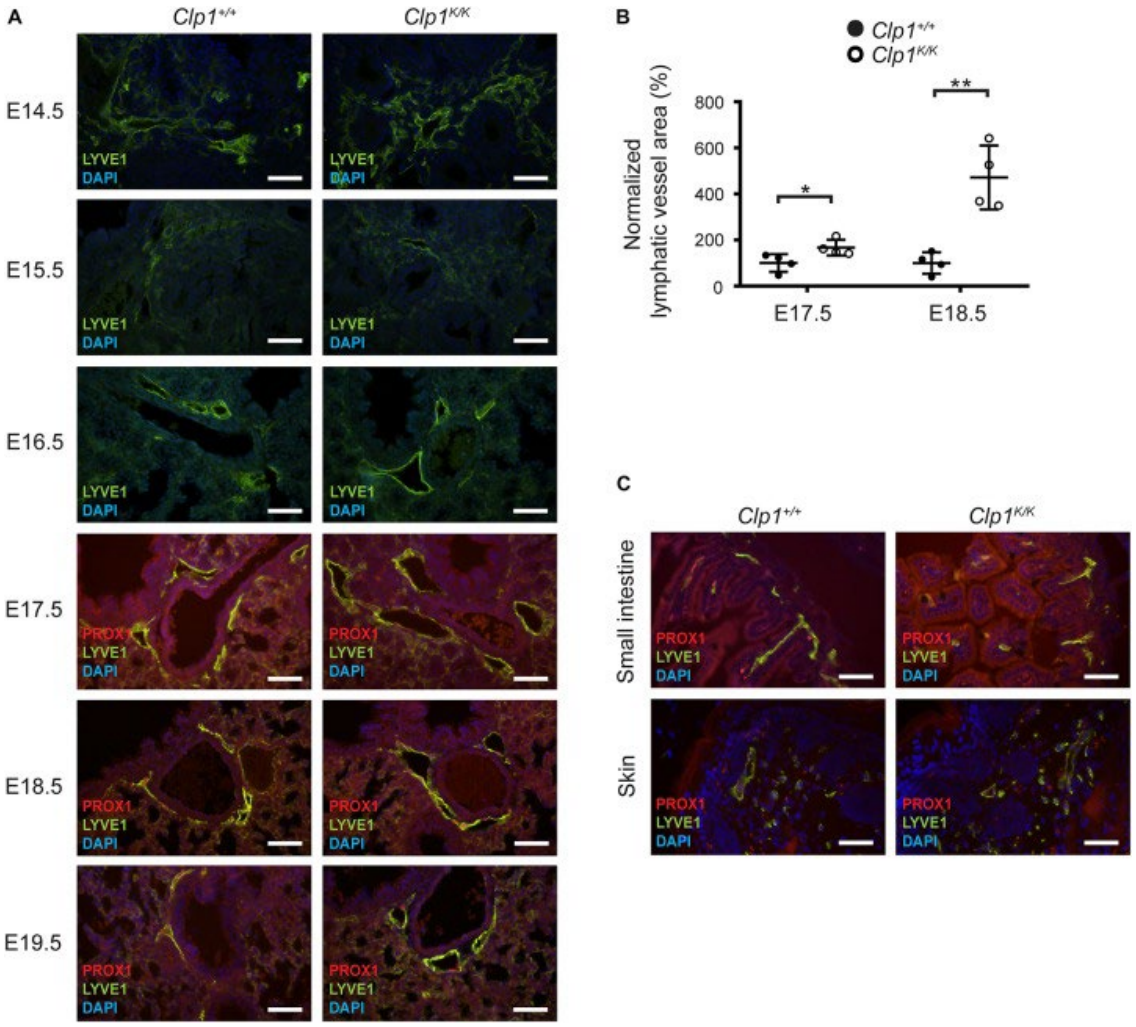

Figure 7 *Dilated pulmonary lymphatic vessels in late gestation Clp1$^{K/K}$ embryos with impaired FBMs (I).*

A) Morphology of lymphatic vessels shown by immunostaining for LYVE1, PROX1 lymphatic markers and DAPI nuclear staining at different stages of embryonic life (E14.5, E15.5, 16.5, E17.5, E18.5 and E19.5) of *Clp1*$^{+/+}$ and *Clp1*$^{K/K}$ embryonic lungs on the c57Bl/6 genetic background. Representative images are shown of 2-4 embryos per each group. Bars, 50µm. **B**) Normalized lymphatic vessel area in *Clp1*$^{+/+}$ and *Clp1*$^{K/K}$ embryos at E17.5 and E18.5 before birth on the c57Bl/6 genetic background. Quantitative data are shown as mean and SEM of 4 embryos in each group from 3 litters (*P<0.05 (two-tailed t-test)). **C**) Lymphatic morphology of the skin and small intestine shown by immunostaining for LYVE1, PROX1 and nuclear DAPI staining of *Clp1*$^{+/+}$ and *Clp1*$^{K/K}$ embryos at E18.5 on the c57Bl/6 genetic background. Representative images are shown of 4 embryos from 3 litters. Bars, 50µm.

4.5 Lymphatic Function Impairment Shown in Late Gestation Lungs of *Clp1*$^{K/K}$ Embryos

To monitor the lymphatic function, we crossed lymphatic reporter mice (*Flt4*^{YFP}) with Clp1 mice. Large molecular weight (70 kDa) fluorescent labeled macromolecule (RhD) was injected into the developing lung of these mouse embryos. In this experiment after 60 min post injection, we detected selective uptake and transport of the fluorescently labeled macromolecules in reporter positive pulmonary lymphatic vessels in *Clp1*$^{K/+}$ control embryos. Interestingly, we identified decreased RhD signal in the lymphatic vessels of late gestation (E18.5) *Clp1*$^{K/K}$ embryos compared to the controls. These results indicate that lymphatic function was severely reduced in *Clp1*$^{K/K}$ embryos at E18.5 compared to littermate controls (*P = 0.0151) (Figure 8A, B).

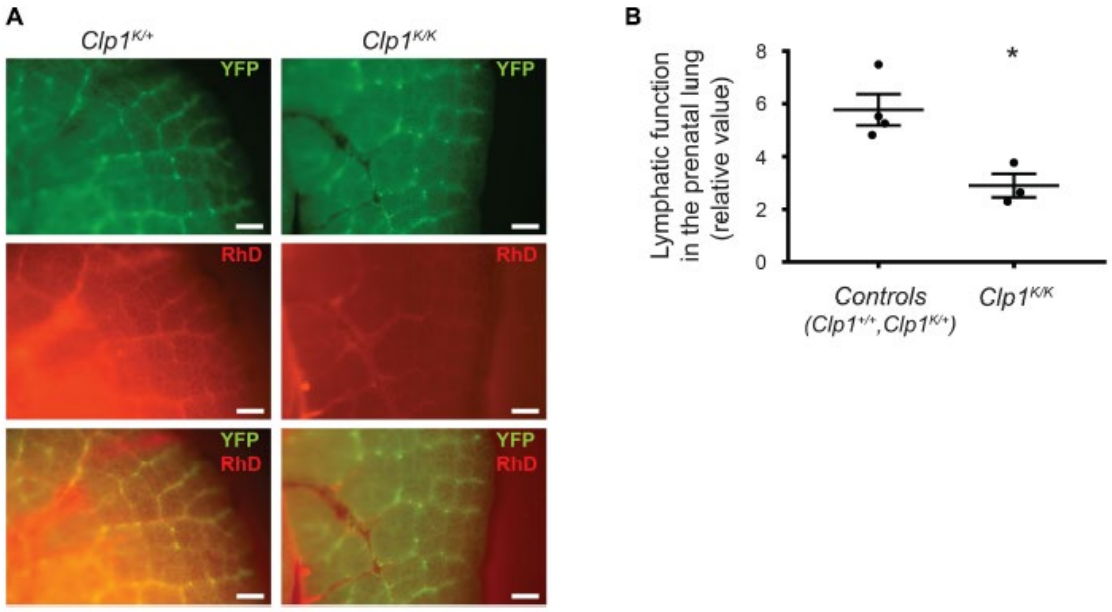

Figure 8 *Impaired pulmonary lymphatic function in late gestation Clp1*$^{K/K}$ *embryos with impaired FBMs (I).*

A) Lymphatic function of late gestation lungs. Monitoring the uptake and transport of fluorescently labelled macromolecules by pulmonary lymphatic vessels in control (*Clp1*$^{+/+}$ or *Clp1*$^{K/+}$) and *Clp1*$^{K/K}$ E18.5 embryonic lungs carrying *Flt4*^{YFP} lymphatic reporter allele on the c57Bl/6 genetic background. The fluorescently labelled macromolecules were 70 kDa RhD which was injected into the lung via the chest wall and uterus. Representative images are shown of 3-4 embryos per group from 5 litters. Bars, 250µm. **B)** Quantitative data for normalized lymphatic function measured as intensity of the RhD signal in fluorescently labelled pulmonary lymphatic vessels are shown as mean and SEM at E18.5 in control (*Clp1*$^{+/+}$, *Clp1*$^{K/+}$) and *Clp1*$^{K/K}$ embryos from 3-4 embryos per each group from 5 litters (*P<0.05 (two-tailed t-test)).

4.6 Local lymphatic growth in vivo by administration of VEGFC mRNA-LNPs into back skin

To characterize organ-specific lymphatic growth in the skin we used *Prox1*^{GFP} lymphatic reporter mice, in which lymphatic endothelial cells express GFP (100). As described in the methods Norbert Pardi from the University of Pennsylvania designed and produced the nucleoside-modified mRNAs and Acuitas Therapeutics, Vancouver, BC, Canada developed and prepared the lipid nanoparticles. These nucleoside-modified VEGFC mRNA-LNPs were injected intradermally into the back skin of *Prox1*^{GFP} lymphatic reporter mice. Remarkably, a major increase in lymphatic growth was detected after 22 days which is shown by fluorescent stereo microscopy by detecting the Prox1-GFP signal (green) and LYVE1 (magenta) expression of lymphatic endothelial cells in paraffin-based histology slides (Figure 9).

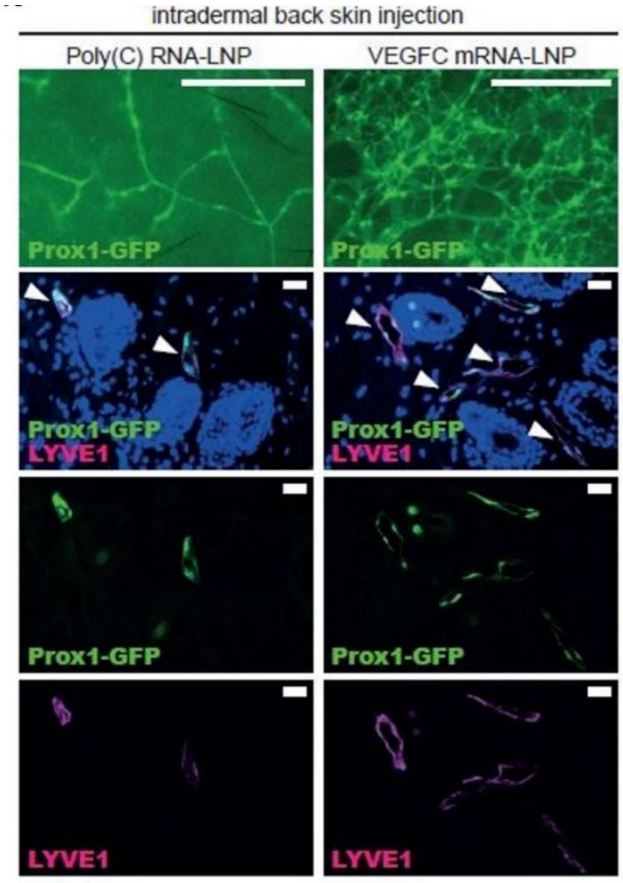

Figure 9 *Lymphatic morphology in the back skin of lymphatic reporter animals injected with control Poly(C) or VEGFC mRNA-LNPs (II).*

Representative images of 15 mice 22 days after the treatment in *Prox1*^{GFP} reporter adult mice are shown by whole-mount fluorescent stereo microscopy (top panels; bars, 1000

μm) and anti-LYVE1 immunostaining of slides processed by paraffin-based histology (lower panels; bars, 50 μm). Arrows show LYVE1 (magenta) and Prox1-GFP(green) positive lymphatic vessels. On the left side the control Poly(C) injected mice have been seen while on the right side *VEGFC mRNA-LNPs* injected mice.

5. Discussion

Besides the well-known, classical functions of lymphatic system, it has become progressively clear that lymphatic vessels, present in different organ-specific environments, has organ specific lymphatic functions (41, 89, 93, 102-104). Our aim was to identify these organ-specific functions of lymphatics, focusing on the neonatal lung and adult skin.

Lung development requires a complex prenatal pulmonary maturation program which prepares the lung for air inflation and gas exchange at birth. All the members and factors of this complicated process are still not fully known. Experimental data indicates surfactant has a key role here, which increases lung compliance by reducing surface tension in the lung (21-24). Therefore, surfactant in therapy improves pulmonary compliance, reduces RDS morbidity and lowers the risk of chronic lung disease (17-20). However, surfactant therapy also has limitations. Therefore, premature newborns still need further supportive care such as oxygen and mechanical ventilation which have long-term complications (35, 36). Thus, new methods and mechanisms would be greatly needed. Therefore, further studies also are needed to uncover other potential therapeutic targets.

Lymphatics of the lung play a critical role in adulthood, for example in diseases such as asthma, tuberculosis, and chronic obstructive pulmonary disease (COPD) (40, 105-108). Remodeling of lung lymphatic vessels have been seen in asthma (109), which is mediated by factors such as VEGFC in addition to other molecules (110, 111). In patients with advanced COPD increased lymphatic vessel density is associated with the alveolar spaces (112) as well as an increased number of lymphoid follicles were found (113). Rather than a passive tube, the lymphatic vasculature is increasingly identified as modulating organ function and disease pathogenesis. Certainly, changes in lymphatic morphology or function have been observed in nearly every lung disease in which they have been studied (43). Novel tools for investigating the lymphatic system contribute to better understanding of their role in diseases and their organ specific functions.

Lungs develop in a fluid environment in utero, the removal of this fluid and the inflation of the lungs are critical steps at the moment of birth. However, early studies do not support significantly increased lymphatic drainage from the lung during or immediately after birth in lambs (54). Prior study of our research group revealed that

lymphatic function increases lung compliance before birth and supports the successful inflation of the lung and also changes lung mechanics to prepare for inflation at birth (38). This poses the question whether it is possible to stimulate the lymphatic function in the lungs before or at birth and what other mechanisms can play role in the lungs to prepare for the first breath.

In utero fetuses perform periodic breathing-like movements during late gestation, these are the fetal breathing movements (FBMs). However, the physiological importance of these events is still not clear. As we search for new mechanisms in preparation of the developing lungs for inflation at birth, better understanding of physiological role of FBMs in this context is needed.

Prior experimental approaches to study FBMs had major limitations. Surgical approaches affect a number of other physiological processes, not just FBMs (76, 77). The leakage or drainage of the amniotic fluid influences the volume and function of the organs in addition to FBMs (78-80). Embryos paralyzed from the early embryonic period such as *Myf5*$^{-/-}$ mice and *Myf5*$^{-/-}$*:MyoD*$^{-/-}$ double knock out mice, have severe defects of the skeletomuscular system represented in their smaller size and reduced growth (71, 72, 75), which also poses serious limitations.

For our experiments we used the *Clp1*$^{K/K}$ kinase-dead mouse model which was described by Hanada et al., 2013 and these mice lose the innervation of skeletal muscles from E16.5 onward. Our results confirmed their findings (84) where *Clp1*$^{K/K}$ newborns showed impaired motor function (including fetal breathing movements) resulting in fatal respiratory failure with cyanosis after birth (Figure 4A, B). It has been reported that the frequency of fetal breathing movements of the late gestation embryos correlates well with the breathing activity of the newborns after birth (60). It is known that embryos paralyzed from the early embryonic period have severe defects of the skeleton represented in their smaller size and reduced growth (71, 72, 75), which results in great experimental limitations. Therefore, we measured the total weight of *Clp1*$^{K/K}$ newborns, and no difference was found. Moreover, there was no difference in size between *Clp1*$^{K/K}$ newborns and control *Clp1*$^{K/+}$ or *Clp1*$^{+/+}$ (Figure 4A, B). Consequently, our results indicate that the *Clp1*$^{K/K}$ mice serve as an excellent genetic model to study the possible role of FBMs on pulmonary development in utero.

In the study of Hanada et al. they examined whether lung development was impaired in *Clp1*$^{K/K}$ mice. Therefore, they investigated Caveolin 1, Surfactant protein A and Surfactant protein C expression which appeared normal indicating normal lung development (84). In connection, we aimed to investigate cellular and molecular lung development in more detail. Therefore, we performed histological analyses and immunohistochemistry studies. The expression of molecular markers of lung development including alveolar type I and II cell, Club cell, mesenchymal cell, and vascular cell markers showed normal pulmonary development (Figure 5). This data corresponds to the previous report where the *Clp1*$^{K/K}$ mouse strain was described, they had similar findings regarding lung development markers Caveolin 1 (alveolar type I cell), Surfactant protein A and Surfactant protein C (alveolar type II cell) (84). Another prior study, in which authors studied the possible role of the mechanical forces on lung development by aspirating the amniotic fluid is indicated that amniotic fluid inhalation influences alveolar type I cell differentiation, where fibroblast growth factor 10 **(**FGF10) and extracellular signal-regulated kinase 1 and 2 (ERK1/2) signaling involved to specify alveolar type II fate (114). In connection with this study, it is relevant to highlight that the leakage or drainage of the amniotic fluid may affect not only FBMs but also the volume and function of the organs. Therefore, this model provides important results about the possible role of mechanical forces and fluid volumes on lung development, however these have serious limitations regarding characterizing the physiological role of FBMs.

However, our data showed impaired lung expansion represented as the alveolar septa being thicker, and the alveolar area is reduced in *Clp1*$^{K/K}$ late gestation embryos which suggest that mechanical forces including FBMs influence the expansion of the developing lung (Figure 6A-C). Former studies, where also FBMs were studied, in connection with indicated defect of lung expansion, were models with transection of the spinal cord or the section of the phrenic nerve. In these studies, the presence of lung hypoplasia was concluded, while part of the results indicated that the cellularity represented by the total DNA content of the developing lung is not affected (76, 77). As referred to their result of total DNA content, we concluded similar findings (Figure 6D). However, the surgical approaches in these former studies manipulating the spinal cord or phrenic nerve are heroic studies and may affect a multitude of other physiological processes in addition to FBMs which poses severe limitations.

Our aim was to describe pulmonary lymphatic growth and function in late gestation *Clp1*$^{K/K}$ embryos. Pulmonary lymphatics are present in the lungs of *Clp1*$^{K/K}$ embryos, but they are markedly dilated at late gestation (Figure 7). Furthermore, late gestation *Clp1*$^{K/K}$ embryos show reduced prenatal lymphatic function as well (Figure 8). Prior studies indicated that prenatal lymphatic function parallelly also plays an important role in preparation of the developing lung for inflation at birth. In this study lymphatic deficient mice were used (*Ccbe1*$^{-/-}$ and *Vegfr3*$^{kd/kd}$), and newborns similarly to *Clp1*$^{K/K}$ newborn was cyanotic and died due to respiratory failure shortly after birth. Furthermore, the lungs of late gestation *Ccbe1*$^{-/-}$ and *Vegfr3*$^{kd/kd}$ embryos also showed thickened alveolar septa and reduced alveolar area. Taken together, our results in accordance with previous findings, all suggest that lymphatics and FBMs have critical role in lungs during prenatal preparation for the first breath. *Ccbe1*$^{-/-}$ *and Vegfr3*$^{kd/kd}$ mice lacking lymphatic function exhibit significant decrease in the compliance compared with control littermates (38). Lymphatics drain the interstitial fluid. All this data suggests that dilated lymphatic vessels as impaired lymphatic function may contribute to the appearance of thickened alveolar septa and reduced alveolar area. In conclusion, our current study confirmed previous findings that lymphatics play an important role in lung development for the preparation to the first breath.

As it was discussed in the introduction, collecting lymphatics in the lung lack smooth muscle cell coverage (39, 40) while other collecting lymphatics in the body has to support the lymph flow. Therefore, in the lung other mechanisms should be present to provide the pumping function and maintain the lymph flow in pulmonary lymphatics. Our result suggests that changes in the pressure and respiratory movements may be a driver of lymphatic drainage in the lung as opposed to the contraction of the vessel itself. These findings suggest that lymphatic function, both pre- and postnatally may be dependent on breathing movements. Therefore, it is possible that FBMs stimulate prenatal lymphatic function in pulmonary collecting lymphatics lacking smooth muscle coverage to prepare the developing lung for inflation and gas exchange at birth. However further investigations are needed to better understand the role of FBMs and lymphatic function in lung development in preparation for the first breath.

It has been recently reported that mechanical pressure-mediated c-JUN (jun proto-oncogene, AP-1 (activating protein-1) transcription factor subunit) expression modulates

remodeling of the actin cytoskeleton in LECs to open flaps which is essential in enabling lymphatic vessels to take up interstitial fluid in P0 lungs (115). They used single cell RNA sequencing analysis which revealed c-JUN transcription factor is transiently upregulated in lymphatic endothelial cells of newborns lungs. In *Jun cKO* and short interfering ribonucleic acid (siRNA) silenced c-JUN (siJUN) models they showed impaired lymphatic vessel opening, which lead fluid retention in the lung and caused the death of newborns. They also confirmed that increased mechanical pressure induces the expression of c-JUN in lymphatic endothelial cells. Moreover, the density of actin fibers decreases in LECs of *siJUN* lungs (115). After these new findings the study of the c-JUN pathway in mice lacking FBMs could provide further valuable information. In this way we could learn more about c-JUN pathway related to fetal breathing movements.

To identify organ specific lymphatic function, next to the study of the neonatal lung, our aim was to investigate lymphatic growth in the skin. Nucleoside-modified mRNA-LNP is a novel, greatly effective, and safe therapeutic tool which is used widely for example for vaccine development, protein replacement therapy, and gene editing (95-98, 116). In these experiments we demonstrated that nucleoside-modified VEGFC-encoding mRNA-LNPs were highly efficient to induce the growth of lymphatic vessels in the back skin of adult mice (Figure 9). These findings may contribute to the treatment of lymphedemas.

Lymphatic vessels are present in different organ-specific environments, which may require different lymphatic growth and function. Neonatal lung and adult skin are immensely different organs. Our aim was to identify organ-specific functions of lymphatics focusing on these two organs. Our results indicated that FBMs have a role in the preparation of the developing lung for the inflation and gas exchange at birth. Furthermore, our current study has confirmed previous findings that lymphatics play an important role in lung development for the preparation to the first breath. These findings suggest that lymphatic function, both pre- and postnatally may be dependent on breathing movements. However, new questions rise and further investigations are needed to better understand the role or FBMs and lymphatic function in lung development in the preparation for the first breath.

6. Conclusions

Surfactants have been considered the most important factors in lung development to prepare the lung for air inflation at birth. A prior study of our research group has reported that lymphatic function is a previously unknown factor which increases lung compliance before birth. Therefore, lymphatics have an important role in preparation for the inflation at birth. We aimed to better understand what other factors and mechanisms could play role in late gestation and at birth. We could confirm that newborns of *Clp1*$^{K/K}$ mice exhibited impaired motility and respiration, or a complete lack of movement and breathing (Figure 4). We think this model is excellent for studying the impact of FBMs on lung development and gives another view compared to previous other approaches like leakage or drainage of the amniotic fluid, performing heroic surgery, or paralysis starting at an early developmental stage, etc., which all have great limitations.

Our next aim was to describe cellular and molecular lung development of *Clp1*$^{K/K}$ late gestation embryos lacking FMBs. We could conclude that it was normal, and no significant difference was detectable between *Clp1*$^{K/K}$ and control *Clp1*$^{+/+}$mice (Figure 5). However, our results demonstrated impaired lung expansion represented in thicker alveolar septa, reduced alveolar area in *Clp1*$^{K/K}$ late gestation embryos which indicates that mechanical forces including FBMs may affect the expansion of the developing lung (Figure 6A-C).

Our following aim was to characterize the lymphatic function in late gestation embryos lacking FBMs. Pulmonary lymphatics are developing and are present in the lungs of *Clp1*$^{K/K}$ embryos, but they are markedly dilated at late gestation (Figure 7). Importantly, late gestation *Clp1*$^{K/K}$ embryos show reduced prenatal lymphatic function as well (Figure 8). Therefore, our results indicate that lymphatics play an important role in lung development for the preparation to the first breath.

Another aspect which could provide valuable information in the future is to stimulate FBMs during late gestation to study whether it could be an effective way to reduce the risk of the development of neonatal respiratory failure.

Our final objective was to characterize a system to induce organ specific lymphatic growth in the skin. With nucleoside-modified VEGFC mRNA-LNP platform we could effectively increase local lymphatic growth in the back skin dose dependently (Figure 9). In the future it may open new aspects of the treatment of lymphedemas**.**

New results in points:

- Our results show impaired lung expansion represented as the alveolar septa are thicker, and the alveolar area is reduced in *Clp1*$^{K/K}$ late gestation embryos.
- Our findings suggest that mechanical forces including FBMs influence the expansion of the developing lung, while the expression of molecular markers of lung development are not affected. We could not detect lung hypoplasia.
- *Clp1*$^{K/K}$ late gestation embryos have dilated pulmonary lymphatic vessels, display reduced prenatal lymphatic function and impaired lung expansion. Our results have revealed the previously unrecognized role of skeletal muscle function including FBMs in prenatal lung expansion, suggesting that FBMs and prenatal pulmonary lymphatics function together to prepare the developing lung for inflation and gas exchange at birth.
- We developed a system to induce organ-specific lymphatic growth in the skin. Nucleoside-modified VEGFC mRNA-LNPs effectively increased local lymphatic growth in back skin.

7. Summary

The classical function of lymphatics such as maintaining tissue homeostasis and immunosurveillance are well known. However, different organs have profoundly different tissue environments, which require organ-specific lymphatic function and growth. Our aim was to better understand organ specific lymphatic function of the neonatal lung and the organ specific lymphatic growth of the adult skin.

Initially, we focused on identifying which mechanisms besides surfactant contribute to preparing the neonatal lung for the first breath. Recently lymphatic function was revealed as a previously unknown mechanical regulator of prenatal lung compliance which prepares the embryonic lung for inflation at birth. Late gestation embryos perform episodic breathing-like movements called fetal breathing movements (FBMs), but the physiological importance of these events is not clear. In our current study we aimed to characterize the physiological role of FBMs in preparation for air inflation at birth. For our experiments we used *Clp1*$^{K/K}$ mice, which develop a progressive loss of spinal motor neurons associated with axonal degeneration and denervation of neuromuscular junctions from E16.5 onward serving as an ideal genetic model to test the possible role of FBMs. We confirmed that *Clp1*$^{K/K}$ newborns showed impaired motor function including FBMs which resulted in fatal respiratory failure after birth. Next, we showed that the alveolar septa are thicker, and the alveolar area is reduced in *Clp1*$^{K/K}$ late gestation embryos, while the expression of molecular markers of lung development is not affected. Importantly, our results have revealed that *Clp1*$^{K/K}$ embryos display dilated pulmonary lymphatic vessels and reduced prenatal lymphatic function and impaired lung expansion. Collecting lymphatics in the lung lack smooth muscle cell coverage, our findings suggest a possible mechanism where FBMs stimulate prenatal lymphatic flow in these pulmonary collecting lymphatics to prepare the developing lung for inflation and gas exchange at birth. Moreover, these results raise the possibility that stimulating FBMs during late gestation might be an effective way to reduce the risk of neonatal respiratory failure.

To better understand organ-specific lymphatic function, we aimed to develop an efficient system to induce lymphatic growth in the skin of adult mice. Our results of experiments with nucleoside-modified VEGFC mRNA LNP platform suggest that this is a novel, greatly potent, and safe therapeutic tool which effectively increases lymphatic growth in the skin of adult mice.

8. References

1. Nikolić MZ, Sun D, Rawlins EL. Human lung development: recent progress and new challenges. Development. 2018;145(16):dev163485.
2. Khoor A, Gray ME, Singh G, Stahlman MT. Ontogeny of Clara cell-specific protein and its mRNA: their association with neuroepithelial bodies in human fetal lung and in bronchopulmonary dysplasia. Journal of Histochemistry & Cytochemistry. 1996;44(12):1429-38.
3. Kitaoka H, Burri PH, Weibel ER. Development of the human fetal airway tree: Analysis of the numerical density of airway endtips. The Anatomical Record. 1996;244(2):207-13.
4. de Vries JI, Visser GH, Prechtl HF. Fetal behaviour in early pregnancy. Eur J Obstet Gynecol Reprod Biol. 1986;21(5-6):271-6.
5. Oulton M, Martin TR, Faulkner GT, Stinson D, Johnson JP. Developmental Study of a Lamellar Body Fraction Isolated From Human Amniotic Fluid. Pediatric Research. 1980;14(5):722-8.
6. Schittny JC. Development of the lung. Cell and Tissue Research. 2017;367(3):427-44.
7. Morrisey EE, Hogan BLM. Preparing for the First Breath: Genetic and Cellular Mechanisms in Lung Development. Developmental Cell. 2010;18(1):8-23.
8. Mullassery D, Smith NP. Lung development. Semin Pediatr Surg. 2015;24(4):152-5.
9. Whitsett JA, Kalin TV, Xu Y, Kalinichenko VV. Building and Regenerating the Lung Cell by Cell. Physiological Reviews. 2019;99(1):513-54.
10. Ersch J, Roth-Kleiner M, Baeckert P, Bucher HU. Increasing incidence of respiratory distress in neonates. Acta Paediatrica. 2007;96(11):1577-81.
11. Parkash A, Haider N, Khoso ZA, Shaikh AS. Frequency, causes and outcome of neonates with respiratory distress admitted to Neonatal Intensive Care Unit, National Institute of Child Health, Karachi. J Pak Med Assoc. 2015;65(7):771-5.
12. Pramanik AK, Rangaswamy N, Gates T. Neonatal Respiratory Distress. Pediatric Clinics of North America. 2015;62(2):453-69.

13. Qian LL, Liu CQ, Guo YX, Jiang YJ, Ni LM, Xia SW, et al. Current status of neonatal acute respiratory disorders: a one-year prospective survey from a Chinese neonatal network. Chin Med J (Engl). 2010;123(20):2769-75.

14. Sweet LR, Keech C, Klein NP, Marshall HS, Tagbo BN, Quine D, et al. Respiratory distress in the neonate: Case definition & guidelines for data collection, analysis, and presentation of maternal immunization safety data. Vaccine. 2017;35(48 Pt A):6506-17.

15. Stevens TP, Sinkin RA. Surfactant replacement therapy. Chest. 2007;131(5):1577-82.

16. Mahoney AD, Jain L. Respiratory disorders in moderately preterm, late preterm, and early term infants. Clin Perinatol. 2013;40(4):665-78.

17. Couser RJ, Ferrara TB, Ebert J, Hoekstra RE, Fangman JJ. Effects of exogenous surfactant therapy on dynamic compliance during mechanical breathing in preterm infants with hyaline membrane disease. J Pediatr. 1990;116(1):119-24.

18. Nouraeyan N, Lambrinakos-Raymond A, Leone M, Sant'Anna G. Surfactant administration in neonates: A review of delivery methods. Can J Respir Ther. 2014;50(3):91-5.

19. Polin RA, Carlo WA, Papile L-A, Polin RA, Carlo W, Tan R, et al. Surfactant Replacement Therapy for Preterm and Term Neonates With Respiratory Distress. Pediatrics. 2014;133(1):156-63.

20. Soll RF. Synthetic surfactant for respiratory distress syndrome in preterm infants. Cochrane Database Syst Rev. 2000;1998(2):CD001149.

21. Christmann U, Buechner-Maxwell VA, Witonsky SG, Hite RD. Role of lung surfactant in respiratory disease: current knowledge in large animal medicine. J Vet Intern Med. 2009;23(2):227-42.

22. Avery ME, Mead J. Surface properties in relation to atelectasis and hyaline membrane disease. AMA J Dis Child. 1959;97(5, Part 1):517-23.

23. Bernhard W. Lung surfactant: Function and composition in the context of development and respiratory physiology. Ann Anat. 2016;208:146-50.

24. Morgan TE. Pulmonary surfactant. N Engl J Med. 1971;284(21):1185-93.

25. Frerking I, Günther A, Seeger W, Pison U. Pulmonary surfactant: functions, abnormalities and therapeutic options. Intensive Care Medicine. 2001;27(11):1699-717.

26. Wright JR. Clearance and recycling of pulmonary surfactant. Am J Physiol. 1990;259(2 Pt 1):L1-12.
27. Wright JR. Immunoregulatory functions of surfactant proteins. Nature Reviews Immunology. 2005;5(1):58-68.
28. Kuroki Y, Voelker DR. Pulmonary surfactant proteins. J Biol Chem. 1994;269(42):25943-6.
29. Tokieda K, Whitsett JA, Clark JC, Weaver TE, Ikeda K, McConnell KB, et al. Pulmonary dysfunction in neonatal SP-B-deficient mice. Am J Physiol. 1997;273(4):L875-82.
30. Weaver TE, Conkright JJ. Function of Surfactant Proteins B and C. Annual Review of Physiology. 2001;63(1):555-78.
31. Whitsett JA, Weaver TE. Hydrophobic Surfactant Proteins in Lung Function and Disease. New England Journal of Medicine. 2002;347(26):2141-8.
32. Keating E, Rahman L, Francis J, Petersen A, Possmayer F, Veldhuizen R, et al. Effect of cholesterol on the biophysical and physiological properties of a clinical pulmonary surfactant. Biophys J. 2007;93(4):1391-401.
33. Orgeig S, Daniels CB, Johnston SD, Sullivan LC. The pattern of surfactant cholesterol during vertebrate evolution and development: does ontogeny recapitulate phylogeny? Reprod Fertil Dev. 2003;15(1-2):55-73.
34. Hills, Chen. Suppression of neural activity of bronchial irritant receptors by surface-active phospholipid in comparison with topical drugs commonly prescribed for asthma. Clinical & Experimental Allergy. 2000;30(9):1266-74.
35. Hintz SR, Poole WK, Wright LL, Fanaroff AA, Kendrick DE, Laptook AR, et al. Changes in mortality and morbidities among infants born at less than 25 weeks during the post-surfactant era. Arch Dis Child Fetal Neonatal Ed. 2005;90(2):F128-33.
36. Suresh GK, Soll RF. Overview of surfactant replacement trials. J Perinatol. 2005;25 Suppl 2:S40-4.
37. Petrova TV, Koh GY. Biological functions of lymphatic vessels. Science. 2020;369(6500).
38. Jakus Z, Gleghorn JP, Enis DR, Sen A, Chia S, Liu X, et al. Lymphatic function is required prenatally for lung inflation at birth. Journal of Experimental Medicine. 2014;211(5):815-26.

39. Baluk P, Fuxe J, Hashizume H, Romano T, Lashnits E, Butz S, et al. Functionally specialized junctions between endothelial cells of lymphatic vessels. The Journal of Experimental Medicine. 2007;204(10):2349-62.
40. Reed HO, Wang L, Sonett J, Chen M, Yang J, Li L, et al. Lymphatic impairment leads to pulmonary tertiary lymphoid organ formation and alveolar damage. Journal of Clinical Investigation. 2019;129(6):2514-26.
41. Aspelund A, Robciuc MR, Karaman S, Makinen T, Alitalo K. Lymphatic System in Cardiovascular Medicine. Circ Res. 2016;118(3):515-30.
42. Kukk E, Lymboussaki A, Taira S, Kaipainen A, Jeltsch M, Joukov V, et al. VEGF-C receptor binding and pattern of expression with VEGFR-3 suggests a role in lymphatic vascular development. Development. 1996;122(12):3829-37.
43. Trivedi A, Reed HO. The lymphatic vasculature in lung function and respiratory disease. Frontiers in Medicine. 2023;10.
44. Breiteneder-Geleff S, Soleiman A, Kowalski H, Horvat R, Amann G, Kriehuber E, et al. Angiosarcomas express mixed endothelial phenotypes of blood and lymphatic capillaries: podoplanin as a specific marker for lymphatic endothelium. Am J Pathol. 1999;154(2):385-94.
45. Banerji S, Ni J, Wang SX, Clasper S, Su J, Tammi R, et al. LYVE-1, a new homologue of the CD44 glycoprotein, is a lymph-specific receptor for hyaluronan. J Cell Biol. 1999;144(4):789-801.
46. Karkkainen MJ, Haiko P, Sainio K, Partanen J, Taipale J, Petrova TV, et al. Vascular endothelial growth factor C is required for sprouting of the first lymphatic vessels from embryonic veins. Nature Immunology. 2004;5(1):74-80.
47. Ober EA, Olofsson B, Makinen T, Jin SW, Shoji W, Koh GY, et al. Vegfc is required for vascular development and endoderm morphogenesis in zebrafish. EMBO Rep. 2004;5(1):78-84.
48. Gordon K, Schulte D, Brice G, Simpson MA, Roukens MG, van Impel A, et al. Mutation in vascular endothelial growth factor-C, a ligand for vascular endothelial growth factor receptor-3, is associated with autosomal dominant milroy-like primary lymphedema. Circ Res. 2013;112(6):956-60.

49. Irrthum A, Karkkainen MJ, Devriendt K, Alitalo K, Vikkula M. Congenital hereditary lymphedema caused by a mutation that inactivates VEGFR3 tyrosine kinase. Am J Hum Genet. 2000;67(2):295-301.

50. Jeltsch M, Jha SK, Tvorogov D, Anisimov A, Leppanen VM, Holopainen T, et al. CCBE1 enhances lymphangiogenesis via A disintegrin and metalloprotease with thrombospondin motifs-3-mediated vascular endothelial growth factor-C activation. Circulation. 2014;129(19):1962-71.

51. Jha SK, Rauniyar K, Karpanen T, Leppanen VM, Brouillard P, Vikkula M, et al. Efficient activation of the lymphangiogenic growth factor VEGF-C requires the C-terminal domain of VEGF-C and the N-terminal domain of CCBE1. Sci Rep. 2017;7(1):4916.

52. Bui HM, Enis D, Robciuc MR, Nurmi HJ, Cohen J, Chen M, et al. Proteolytic activation defines distinct lymphangiogenic mechanisms for VEGFC and VEGFD. J Clin Invest. 2016;126(6):2167-80.

53. Bland RD. Dynamics of pulmonary water before and after birth. Acta Paediatr Scand Suppl. 1983;305:12-20.

54. Bland RD, Hansen TA, Hazinski TA, Haberkern CM, Bressack MA. Studies of lung fluid balance in newborn lambs. Ann N Y Acad Sci. 1982;384:126-45.

55. Bland RD, McMillan DD. Lung fluid dynamics in awake newborn lambs. J Clin Invest. 1977;60(5):1107-15.

56. Wigle JT, Oliver G. Prox1 Function Is Required for the Development of the Murine Lymphatic System. Cell. 1999;98(6):769-78.

57. Zou Z, Enis DR, Bui H, Khandros E, Kumar V, Jakus Z, et al. The secreted lymphangiogenic factor CCBE1 is essential for fetal liver erythropoiesis. Blood. 2013;121(16):3228-36.

58. Karkkainen MJ, Saaristo A, Jussila L, Karila KA, Lawrence EC, Pajusola K, et al. A model for gene therapy of human hereditary lymphedema. Proceedings of the National Academy of Sciences. 2001;98(22):12677-82.

59. Zhang L, Zhou F, Han W, Shen B, Luo J, Shibuya M, et al. VEGFR-3 ligand-binding and kinase activity are required for lymphangiogenesis but not for angiogenesis. Cell Research. 2010;20(12):1319-31.

60. Niblock MM, Perez A, Broitman S, Jacoby B, Aviv E, Gilkey S. In utero development of fetal breathing movements in C57BL6 mice. Respir Physiol Neurobiol. 2020;271:103288.
61. Harding R. Fetal pulmonary development: the role of respiratory movements. Equine Veterinary Journal. 1997;29(S24):32-9.
62. Govindan RB, Wilson JD, Murphy P, Russel WA, Lowery CL. Scaling analysis of paces of fetal breathing, gross-body and extremity movements. Physica A. 2007;386(1):231-9.
63. Kisilevsky BS, Hains SM, Low JA. Maturation of body and breathing movements in 24-33 week-old fetuses threatening to deliver prematurely. Early Hum Dev. 1999;55(1):25-38.
64. Tendais I, Figueiredo B, Mulder EJH, Lopes D, Montenegro N. Developmental trajectories of general and breathing movements in fetal twins. Developmental Psychobiology. 2019;61(4):626-33.
65. Bots RS, Broeders GH, Farman DJ, Haverkorn MJ, Stolte LA. Fetal breathing movements in the normal and growth-retarded human fetus: a multiscan/M-mode echofetographic study. Eur J Obstet Gynecol Reprod Biol. 1978;8(1):21-9.
66. De Vries JIP, Fong BF. Normal fetal motility: an overview. Ultrasound in Obstetrics & Gynecology. 2006;27(6):701-11.
67. De Vries JIP, Fong BF. Changes in fetal motility as a result of congenital disorders: an overview. Ultrasound in Obstetrics & Gynecology. 2007;29(5):590-9.
68. Feldman JL, Kam K, Janczewski WA. Practice makes perfect, even for breathing. Nature Neuroscience. 2009;12(8):961-3.
69. Greer JJ, Funk GD, Ballanyi K. Preparing for the first breath: prenatal maturation of respiratory neural control. The Journal of Physiology. 2006;570(3):437-44.
70. Inanlou MR, Baguma-Nibasheka M, Kablar B. The role of fetal breathing-like movements in lung organogenesis. Histol Histopathol. 2005;20(4):1261-6.
71. Inanlou MR, Kablar B. Abnormal development of the intercostal muscles and the rib cage in Myf5−/− embryos leads to pulmonary hypoplasia. Developmental Dynamics. 2005;232(1):43-54.

72. Inanlou MR, Kablar B. Contractile activity of skeletal musculature involved in breathing is essential for normal lung cell differentiation, as revealed in Myf5−/−:MyoD−/− embryos. Developmental Dynamics. 2005;233(3):772-82.
73. Perlman M, Williams J, Hirsch M. Neonatal pulmonary hypoplasia after prolonged leakage of amniotic fluid. Archives of Disease in Childhood. 1976;51(5):349-53.
74. Sandler DL, Burchfield DJ, McCarthy JA, Rojiani AM, Drummond WH. Early-onset respiratory failure caused by severe congenital neuromuscular disease. J Pediatr. 1994;124(4):636-8.
75. Tseng BS, Cavin ST, Booth FW, Olson EN, Marin MC, McDonnell TJ, et al. Pulmonary hypoplasia in the myogenin null mouse embryo. Am J Respir Cell Mol Biol. 2000;22(3):304-15.
76. Bamford OS, Rivera A, Tadalan T, Ellis W. Effects of in utero phrenic nerve section on the development of collagen and elastin in lamb lungs. Am Rev Respir Dis. 1992;146(5 Pt 1):1202-5.
77. Fewell JE, Lee CC, Kitterman JA. Effects of phrenic nerve section on the respiratory system of fetal lambs. J Appl Physiol Respir Environ Exerc Physiol. 1981;51(2):293-7.
78. Alcorn D, Adamson TM, Lambert TF, Maloney JE, Ritchie BC, Robinson PM. Morphological effects of chronic tracheal ligation and drainage in the fetal lamb lung. J Anat. 1977;123(Pt 3):649-60.
79. Kotecha S. Lung growth for beginners. Paediatr Respir Rev. 2000;1(4):308-13.
80. Moessinger AC, Harding R, Adamson TM, Singh M, Kiu GT. Role of lung fluid volume in growth and maturation of the fetal sheep lung. Journal of Clinical Investigation. 1990;86(4):1270-7.
81. Ott M-O, Bober E, Lyons G, Arnold H, Buckingham M. Early expression of the myogenic regulatory gene, myf-5, in precursor cells of skeletal muscle in the mouse embryo. Development. 1991;111(4):1097-107.
82. Rudnicki MA, Schnegelsberg PN, Stead RH, Braun T, Arnold HH, Jaenisch R. MyoD or Myf-5 is required for the formation of skeletal muscle. Cell. 1993;75(7):1351-9.

83. Davis RL, Weintraub H, Lassar AB. Expression of a single transfected cDNA converts fibroblasts to myoblasts. Cell. 1987;51(6):987-1000.
84. Hanada T, Weitzer S, Mair B, Bernreuther C, Wainger BJ, Ichida J, et al. CLP1 links tRNA metabolism to progressive motor-neuron loss. Nature. 2013;495(7442):474-80.
85. Paushkin SV, Patel M, Furia BS, Peltz SW, Trotta CR. Identification of a Human Endonuclease Complex Reveals a Link between tRNA Splicing and Pre-mRNA 3′ End Formation. Cell. 2004;117(3):311-21.
86. Yang Y, Wang X, Wang P. Signaling mechanisms underlying lymphatic vessel dysfunction in skin aging and possible anti-aging strategies. Biogerontology. 2023;24(5):727-40.
87. Geng X, Ho Y-C, Srinivasan RS. Biochemical and mechanical signals in the lymphatic vasculature. Cellular and Molecular Life Sciences. 2021;78(16):5903-23.
88. Krouwer VJD, Hekking LHP, Langelaar-Makkinje M, Regan-Klapisz E, Post J. Endothelial cell senescence is associated with disrupted cell-cell junctions and increased monolayer permeability. Vascular Cell. 2012;4(1):12.
89. Alitalo K. The lymphatic vasculature in disease. Nature Medicine. 2011;17(11):1371-80.
90. Mortimer PS, Rockson SG. New developments in clinical aspects of lymphatic disease. J Clin Invest. 2014;124(3):915-21.
91. Radhakrishnan K, Rockson SG. The clinical spectrum of lymphatic disease. Ann N Y Acad Sci. 2008;1131:155-84.
92. Makinen T, Veikkola T, Mustjoki S, Karpanen T, Catimel B, Nice EC, et al. Isolated lymphatic endothelial cells transduce growth, survival and migratory signals via the VEGF-C/D receptor VEGFR-3. EMBO J. 2001;20(17):4762-73.
93. Petrova TV, Koh GY. Organ-specific lymphatic vasculature: From development to pathophysiology. J Exp Med. 2018;215(1):35-49.
94. Pardi N, Tuyishime S, Muramatsu H, Kariko K, Mui BL, Tam YK, et al. Expression kinetics of nucleoside-modified mRNA delivered in lipid nanoparticles to mice by various routes. J Control Release. 2015;217:345-51.
95. Magadum A, Kaur K, Zangi L. mRNA-Based Protein Replacement Therapy for the Heart. Mol Ther. 2019;27(4):785-93.

96. Pardi N, Hogan MJ, Porter FW, Weissman D. mRNA vaccines - a new era in vaccinology. Nat Rev Drug Discov. 2018;17(4):261-79.
97. Sahu I, Haque A, Weidensee B, Weinmann P, Kormann MSD. Recent Developments in mRNA-Based Protein Supplementation Therapy to Target Lung Diseases. Mol Ther. 2019;27(4):803-23.
98. Trepotec Z, Lichtenegger E, Plank C, Aneja MK, Rudolph C. Delivery of mRNA Therapeutics for the Treatment of Hepatic Diseases. Mol Ther. 2019;27(4):794-802.
99. Calvo C-F, Fontaine RH, Soueid J, Tammela T, Makinen T, Alfaro-Cervello C, et al. Vascular endothelial growth factor receptor 3 directly regulates murine neurogenesis. Genes & Development. 2011;25(8):831-44.
100. Choi I, Chung HK, Ramu S, Lee HN, Kim KE, Lee S, et al. Visualization of lymphatic vessels by Prox1-promoter directed GFP reporter in a bacterial artificial chromosome-based transgenic mouse. Blood. 2011;117(1):362-5.
101. Schindelin J, Arganda-Carreras I, Frise E, Kaynig V, Longair M, Pietzsch T, et al. Fiji: an open-source platform for biological-image analysis. Nature Methods. 2012;9(7):676-82.
102. Bálint L, Ocskay Z, Deák BA, Aradi P, Jakus Z. Lymph Flow Induces the Postnatal Formation of Mature and Functional Meningeal Lymphatic Vessels. Frontiers in Immunology. 2020;10.
103. Machnik A, Neuhofer W, Jantsch J, Dahlmann A, Tammela T, Machura K, et al. Macrophages regulate salt-dependent volume and blood pressure by a vascular endothelial growth factor-C–dependent buffering mechanism. Nature Medicine. 2009;15(5):545-52.
104. Oliver G, Kipnis J, Randolph GJ, Harvey NL. The Lymphatic Vasculature in the 21(st) Century: Novel Functional Roles in Homeostasis and Disease. Cell. 2020;182(2):270-96.
105. El-Chemaly S, Levine SJ, Moss J. Lymphatics in lung disease. Ann N Y Acad Sci. 2008;1131:195-202.
106. Mori M, Andersson CK, Graham GJ, Lofdahl CG, Erjefalt JS. Increased number and altered phenotype of lymphatic vessels in peripheral lung compartments of patients with COPD. Respir Res. 2013;14(1):65.

107. Stump B, Cui Y, Kidambi P, Lamattina AM, El-Chemaly S. Lymphatic Changes in Respiratory Diseases: More than Just Remodeling of the Lung? Am J Respir Cell Mol Biol. 2017;57(3):272-9.
108. Summers BD, Kim K, Clement CC, Khan Z, Thangaswamy S, McCright J, et al. Lung lymphatic thrombosis and dysfunction caused by cigarette smoke exposure precedes emphysema in mice. Sci Rep. 2022;12(1):5012.
109. Ebina M. Remodeling of airway walls in fatal asthmatics decreases lymphatic distribution; beyond thickening of airway smooth muscle layers. Allergol Int. 2008;57(2):165-74.
110. Baluk P, Yao LC, Feng J, Romano T, Jung SS, Schreiter JL, et al. TNF-alpha drives remodeling of blood vessels and lymphatics in sustained airway inflammation in mice. J Clin Invest. 2009;119(10):2954-64.
111. Yao LC, Baluk P, Feng J, McDonald DM. Steroid-resistant lymphatic remodeling in chronically inflamed mouse airways. Am J Pathol. 2010;176(3):1525-41.
112. Hardavella G, Tzortzaki EG, Siozopoulou V, Galanis P, Vlachaki E, Avgousti M, et al. Lymphangiogenesis in COPD: another link in the pathogenesis of the disease. Respir Med. 2012;106(5):687-93.
113. Hogg JC, Pare PD, Hackett TL. The Contribution of Small Airway Obstruction to the Pathogenesis of Chronic Obstructive Pulmonary Disease. Physiol Rev. 2017;97(2):529-52.
114. Li J, Wang Z, Chu Q, Jiang K, Li J, Tang N. The Strength of Mechanical Forces Determines the Differentiation of Alveolar Epithelial Cells. Dev Cell. 2018;44(3):297-312 e5.
115. Fu S, Wang Y, Bin E, Huang H, Wang F, Tang N. c-JUN-mediated transcriptional responses in lymphatic endothelial cells are required for lung fluid clearance at birth. Proceedings of the National Academy of Sciences. 2023;120(2).
116. Baden LR, El Sahly HM, Essink B, Kotloff K, Frey S, Novak R, et al. Efficacy and Safety of the mRNA-1273 SARS-CoV-2 Vaccine. N Engl J Med. 2021;384(5):403-16.

9. Bibliography of the candidate's publications

9.1 Publications related to the thesis

I. **Szoták-Ajtay, Kitti**; Szőke, Dániel; Kovács, Gábor; Andréka, Judit; Brenner, Gábor B.; Giricz, Zoltán; Penninger, Josef; Kahn, Mark L.; Jakus, Zoltán Reduced Prenatal Pulmonary Lymphatic Function Is Observed in *Clp1*$^{K/K}$ Embryos With Impaired Motor Functions Including Fetal Breathing Movements in Preparation of the Developing Lung for Inflation at Birth FRONTIERS IN BIOENGINEERING AND BIOTECHNOLOGY 8 Paper: 136 , 15 p. (2020)

II. Szőke, Dániel; Kovács, Gábor; Kemecsei, Éva; Bálint, László; **Szoták-Ajtay, Kitti**; Aradi, Petra; Styevkóné Dinnyés, Andrea; Mui, Barbara L.; Tam, Ying K.; Madden, Thomas D., Karikó, Katalin; Kataru, Raghu, P; Hope, Michael, J; Weissman, Drew; Mehrara, Babak, J; Pardi, Norbert; Jakus, Zoltán Nucleoside-modified VEGFC mRNA induces organ-specific lymphatic growth and reverses experimental lymphedema NATURE COMMUNICATIONS 12 : 1 Paper: 3460 , 18 p. (2021)

9.2 Publications NOT related to the thesis

III. Gara, Edit; Zucchelli, Eleonora; Nemes, Annamária; Jakus, Zoltán; **Ajtay, Kitti**; Kemecsei, Éva; Kiszler, Gábor; Hegedűs, Nikolett; Szigeti, Krisztián; Földes, Iván; Árvai, Kristóf; Kósa, János; Kolev, Kraszimir; Komorowicz, Erzsébet; Padmanabhan, Parasuraman; Maurovich-Horvat, Pál; Dósa, Edit; Várady, György; Pólos, Miklós; Hartyánszky István; Harding, Sian, E; Merkely, Béla; Máthé, Domonkos; Szabó, Gábor; Radovits, Tamás; Földes, Gábor 3D culturing of human pluripotent stem cells-derived endothelial cells for vascular regeneration THERANOSTICS 12 : 10 pp. 4684-4702. , 19 p. (2022)

IV. Tőkési, Natália; Kozák, Eszter; Fülöp, Krisztina; Dedinszki, Dór.; Hegedűs, Nikolett; Király, Bálint; Szigeti, Krisztián; **Ajtay, Kitti**; Jakus, Zoltán; Zaworski, Jeremi; Letavernier, Emmanuel; Pomozi, Viola; Váradi András Pyrophosphate therapy prevents trauma-induced calcification in the mouse model of neurogenic heterotopic ossification JOURNAL OF CELLULAR AND MOLECULAR MEDICINE 24 : 20 pp. 11791-11799. , 9 p. (2020)

V. M-Hamvas, Márta; **Ajtay, Kitti**; Beyer, D ; Jámbrik, Katalin; Vasas, Gábor; Surányi, Gyula; Máthé, Csaba Cylindrospermopsin induces biochemical changes leading to programmed cell death in plants. APOPTOSIS 22 : 2 pp. 254-264. , 11 p. (2017)

∑IF:45.261

10. Acknowledgements

I am grateful to my supervisor, Zoltán Jakus for all of his support and help. I thank Valéria Németh, Éva Kemecsei, Eszter Marinkás and Dorisz Csengel for excellent technical assistance, Petra Aradi, Gábor Kovács and Dániel Szőke for help with experiments, Jean-Léon Thomas (Yale University) for $Flt4^{YFP}$ mice, Zoltán Giricz and Gábor Brenner (Department of Pharmacology and Pharmacotherapy, Semmelweis University), and all member of the Lymphatic Physiology Research Group of Physiology Department. I am grateful to László Hunyady, the former head of Physiology Department and Attila Mócsai, the present head of Physiology Department for the opportunity to work here. I also thank Erzsébet Ligeti, the former head of the Molecular Medicine Division and Péter Várnai, the present head of the Molecular Medicine Division for the opportunity to participate in the PhD program.

Figures 1-3 were created using BioRender.com.

FUNDING:

This work was supported by the Lendület program of the Hungarian Academy of Sciences (LP2014-4/2018), the National Research, Development and Innovation Office (NVKP_16-2016-1-0039), the European Union and the Hungarian Government (VEKOP-2.3.2-16-2016-00002 and VEKOP-2.3.3-15-2016-00006), the Higher Education Institutional Excellence Program of the Ministry for Innovation and Technology in Hungary, within the framework of the Molecular Biology thematic program of the Semmelweis University.